

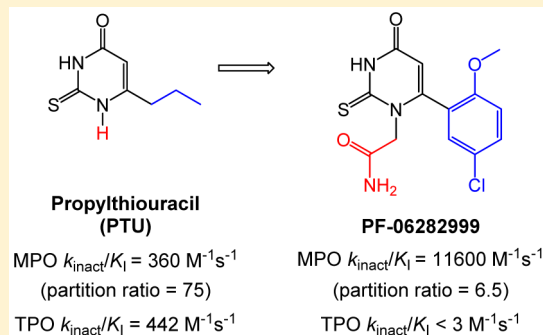
Discovery of 2-(6-(5-Chloro-2-methoxyphenyl)-4-oxo-2-thioxo-3,4-dihydropyrimidin-1(2H)-yl)acetamide (PF-06282999): A Highly Selective Mechanism-Based Myeloperoxidase Inhibitor for the Treatment of Cardiovascular Diseases

Roger B. Ruggeri,* Leonard Buckbinder, Scott W. Bagley, Philip A. Carpino, Edward L. Conn, Matthew S. Dowling, Dilinie P. Fernando, Wenhua Jiao, Daniel W. Kung, Suvi T. M. Orr, Yingmei Qi, Benjamin N. Rocke, Aaron Smith, Joseph S. Warmus, Yan Zhang, Daniel Bowles, Daniel W. Widlicka, Heather Eng, Tim Ryder, Raman Sharma, Angela Wolford, Carlin Okerberg, Karen Walters, Tristan S. Maurer, Yanwei Zhang, Paul D. Bonin, Samantha N. Spath, Gang Xing, David Hepworth, Kay Ahn, and Amit S. Kalgutkar

Worldwide Research and Development, Pfizer, Inc., Groton, Connecticut 06340, United States

ABSTRACT: Myeloperoxidase (MPO) is a heme peroxidase that catalyzes the production of hypochlorous acid. Clinical evidence suggests a causal role for MPO in various autoimmune and inflammatory disorders including vasculitis and cardiovascular and Parkinson's diseases, implying that MPO inhibitors may represent a therapeutic treatment option. Herein, we present the design, synthesis, and preclinical evaluation of N1-substituted-6-arylthiouracils as potent and selective inhibitors of MPO. Inhibition proceeded in a time-dependent manner by a covalent, irreversible mechanism, which was dependent upon MPO catalysis, consistent with mechanism-based inactivation. N1-Substituted-6-arylthiouracils exhibited low partition ratios and high selectivity for MPO over thyroid peroxidase and cytochrome P450 isoforms. N1-Substituted-6-arylthiouracils also demonstrated inhibition of MPO

activity in lipopolysaccharide-stimulated human whole blood. Robust inhibition of plasma MPO activity was demonstrated with the lead compound 2-(6-(5-chloro-2-methoxyphenyl)-4-oxo-2-thioxo-3,4-dihydropyrimidin-1(2H)-yl)acetamide (PF-06282999, **8**) upon oral administration to lipopolysaccharide-treated cynomolgus monkeys. On the basis of its pharmacological and pharmacokinetic profile, PF-06282999 has been advanced to first-in-human pharmacokinetic and safety studies.



INTRODUCTION

Myeloperoxidase (MPO, EC 1.11.2.2) is a member of the heme peroxidase family of enzymes and catalyzes the production of hypochlorous acid (HOCl) from hydrogen peroxide (H_2O_2) and chloride ion (Cl^-). MPO is produced in the bone marrow and stored in the azurophilic granules of neutrophils, where it constitutes up to 5% of the cellular protein; it is also found, albeit to a lesser extent, in some human monocytes and macrophages.¹ Upon phagocyte activation, MPO activity appears within the phagolysosome and extracellularly. The main function of MPO is considered to be microbicidal; however, MPO deficiency occurs in $\sim 1/2000$ individuals² and is not usually associated with increased risk of infections.³

Compelling human data implicate MPO in the pathogenesis of a number of acute and chronic inflammatory diseases such as chronic obstructive pulmonary disease (COPD),⁴ rheumatoid arthritis,⁵ acute kidney injury,⁶ and Parkinson's⁷ and cardiovascular diseases.⁸ The role of MPO in cardiovascular diseases has been particularly well studied in humans; high levels of MPO are found in atherosclerotic plaques, and

elevated plasma MPO levels are associated with risk of major adverse cardiovascular events in otherwise apparently healthy individuals. In addition, elevated MPO levels are also associated with risk of secondary adverse events in stable coronary artery disease subjects, as well as those with recent acute coronary syndrome.^{9,10} Mechanisms by which MPO may contribute to the pathogenesis of diseases include (1) MPO-specific oxidation of lipids and proteins including those in low-density and high-density lipoproteins, contributing to oxidative tissue damage and atherosclerosis,^{11,12} (2) consumption of nitric oxide, thereby impairing nitric oxide-dependent vasodilation, leading to endothelial/vasomotor dysfunction in humans;^{13,14} and (3) microvascular occlusion resulting from the MPO-dependent formation of neutrophil extracellular traps in response to certain stimuli (e.g., phorbol myristate acetate).¹⁵ Studies in MPO deficient mice have demonstrated protection from cardiac remodeling and impaired left ventricular function

Received: June 22, 2015

following surgically induced myocardial infarction.^{16,17} More recently, Churg et al.⁴ have also demonstrated that the MPO inhibitor 3-[[[(2*S*)-tetrahydrofuran-2-yl]methyl]-2-thioxo-7*H*-purin-6-one (AZD-5904,¹⁸ AZ1, or TX4, Figure 1) is able to

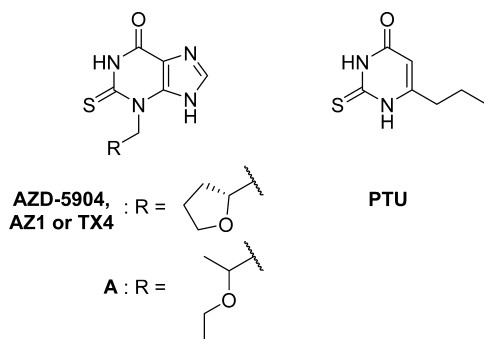


Figure 1. Structures of previously reported MPO irreversible inhibitors.

halt the progression of emphysema and small airway remodeling in a guinea pig model of COPD. In addition, a further MPO inhibitor (AZD-3241) is reported to be currently undergoing clinical trials for the treatment of multiple system atrophy.¹⁹

MPO is a complex hemoprotein with multiple intermediate states (Figure 2). The peroxidation reaction (reaction 1 in Figure 2) involves the native ferric enzyme, which undergoes a two-electron oxidation reaction with H_2O_2 producing the highly reactive form of the enzyme, compound I. In the

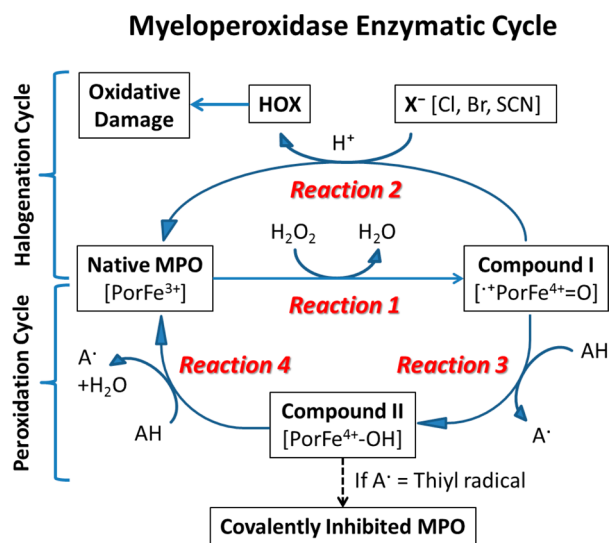


Figure 2. Enzymatic cycle for myeloperoxidase. Oxidation of native MPO by hydrogen peroxide (reaction 1) gives rise to compound I, the most oxidatively reactive state for MPO. In the halogenation cycle (reaction 2) a substrate, typically chloride, undergoes oxidation to afford a reactive species (e.g., hypochlorous acid) that can contribute to tissue damage under inflammatory conditions. In the peroxidation cycle, compound I reacts with an electron-rich organic substrate (reaction 3) to provide a radical species and compound II. For certain substrates such as those described in this article, the resulting radical species may then react with MPO to form a covalent adduct, rendering it irreversibly inhibited. Compound II may also react with another readily oxidized species (reaction 4) to return to the native state of the enzyme and complete the peroxidation cycle.

chlorination (or halogenation) cycle, compound I reacts with chloride (or other halides) through a two-electron reduction reaction to be reduced back to the native enzyme, generating HOCl (or HOX, reaction 2 in Figure 2). Alternatively, in the peroxidation cycle, compound I may oxidize various electron-rich organic substrates including phenols,²⁰ anilines,²¹ and thiols²² (AH) via a one-electron transfer reaction generating the compound II form of the enzyme (reaction 3 in Figure 2). Transfer of an additional electron to compound II from another molecule of the organic substrate, or an alternative source, regenerates native MPO (reaction 4 in Figure 2).

While MPO inhibitors hold much promise as therapeutic agents, their development has been challenging. Many known MPO inhibitors^{20,23} such as hydroxamic acid, indole, hydrazine, aniline, and tryptamine derivatives inhibit the chlorinating activity of MPO in vitro by acting as peroxidase substrates and diverting the enzyme from the chlorinating cycle to the peroxidation cycle. Such compounds promote the formation of compound II by being readily oxidized by compound I (i.e., reaction 3 in Figure 2), one of the strongest oxidizing enzyme intermediates found in vivo, but they do not then react with compound II. Accumulated compound II can be easily reduced back to the native enzyme form by many other electron donors such as urate, ascorbate, tyrosine, or superoxide anion readily found in vivo (i.e., reaction 4 in Figure 2).^{24–28} Thus, in vivo the mode of inhibition by these inhibitors is reversible and likely to be ineffective against HOCl-mediated tissue damage.²⁹ More recently, 2-thioxanthines represented by AZD-5904 (also reported as AZ1 or TX4) and compound A were reported to be mechanism-based inactivators of MPO (Figure 1).^{4,30–32} AZD-5904 and A are suicide substrates of MPO, acting as substrates in reaction 3 in Figure 2 via the one-electron reduction of compound I to compound II followed by covalent modification of the heme moiety by a thiyl radical species generated from AZD-5904 and A in the course of catalysis.^{30–32} The resulting covalent modification of the MPO heme “traps” MPO in an unreactive state, which cannot readily be converted back to the native form, in contrast to the reversible single electron transfer mechanism of inhibition.

In the present manuscript, we describe the design, synthesis, and preclinical characterization of *N*1-substituted-6-aryl-2-thiouracil analogs as novel mechanism-based inhibitors of MPO with high selectivity over thyroid peroxidase (TPO) and over heme-containing cytochrome P450 (CYP) isoforms. The lead compound 2-(6-(5-chloro-2-methoxyphenyl)-4-oxo-2-thioxo-3,4-dihydropyrimidin-1(2*H*)-yl)acetamide (PF-06282999, 8) displayed excellent oral pharmacokinetics in preclinical species and robust irreversible inhibition of plasma MPO activity both in human blood stimulated exogenously and in plasma collected after oral (po) administration to lipopolysaccharide (LPS)-treated cynomolgus monkeys. PF-06282999 has been advanced into first-in-human pharmacokinetics and safety studies.

RESULTS AND DISCUSSION

Selection of in Vitro Assays To Guide Structure–Activity Relationship (SAR) Studies. Propylthiouracil (PTU, Figure 1) is an inhibitor of TPO used clinically for the treatment of hyperthyroidism.³³ Reports on the MPO substrate and inhibitory properties of PTU have been published;^{34–37} however, a detailed kinetic investigation providing evidence for mechanism-based inactivation of MPO has not been reported. To assess the feasibility of PTU as a

potential chemical lead for the de novo design of selective MPO inhibitors, we examined the mechanism of MPO inhibition by PTU in greater detail by measuring MPO peroxidase activity with Amplex Red (10-acetyl-3,7-dihydroxyphenoxazine) as a substrate.³²

As shown in Figure 3A, the MPO reaction with H₂O₂ and Amplex Red was linear over ~500 s in the absence of PTU. However, in the presence of PTU, the progressive curves exhibited curvature and time-dependent inhibition, as typically observed with an irreversible mechanism of inhibition. The data were fit to eq 1, and the rate of MPO inactivation at each inhibitor concentration (k_{obs}) was determined as described in the Experimental Section. Plotting these k_{obs} values as a function of PTU concentration revealed a linear line that passed through near the origin, which was consistent with a two-step inactivation kinetics process when the concentration of inhibitor is far below K_I (Figure 3B). On the basis of this model (eq 3), the slope of the line (which is equal to k_{inact}/K_I , the second-order rate constant and the overall inactivation potency) was determined to be 360 M⁻¹ s⁻¹ for PTU. An IC₅₀ value of 2.81 μM for MPO inhibition was also obtained by using initial rates from the first 300 s of the reaction at each inhibitor concentration (Figure 3C). To verify that the inhibition of MPO by PTU was irreversible and required H₂O₂, we performed rapid dilution experiments in the presence and absence of H₂O₂. After preincubation of MPO with PTU for 15 min, the reaction mixture was rapidly diluted 300-fold into the assay buffer containing both H₂O₂ and Amplex Red substrates, and the resulting recovery of MPO activity was immediately monitored. As shown in Figure 4, no recovery of MPO activity was observed with PTU when H₂O₂ was included in the preincubation mixture, confirming that PTU is an irreversible inhibitor. However, when the rapid dilution experiment was performed in the absence of H₂O₂ substrate during preincubation, MPO activity was recovered to a similar level as that of the DMSO control, indicating MPO catalysis by the substrate H₂O₂ was required for inhibition by PTU. Taken together, these data indicated that PTU is a mechanism-based inhibitor of MPO. TPO inhibition by PTU was evaluated using methods analogous to those above for MPO and the k_{inact}/K_I ratio and IC₅₀ values were determined to be 442 M⁻¹ s⁻¹ and 3.38 μM, respectively, thus demonstrating that PTU is not selective as it inhibits both TPO and MPO with comparable potency.

Although PTU was not selective for inhibition between TPO and MPO, its mechanism-based inhibition profile was deemed suitable for a chemical starting point to identify selective inhibitors, and the assays used in its characterization were adapted for use as primary in vitro screens for inactivation of MPO and for selectivity versus TPO. SAR studies were carried out using the second-order rate constant k_{inact}/K_I ratio as the measure of potency. Unlike IC₅₀ values, k_{inact}/K_I ratios are independent of incubation times and substrate concentrations and are generally considered the best measure of potency for irreversible inhibitors.³⁸

Partition ratio is a quantitative assessment of the efficiency with which mechanism-based inhibitors inactivate their targets. The reactive intermediate that is formed by reaction of an enzyme with a potential mechanism-based inhibitor may either (a) directly form a covalent adduct in the enzyme active site (resulting in inactivation) or (b) escape from the active site (leaving enzyme activity intact). PTU was found to have a high partition ratio of 75 for inhibition of MPO, meaning that the

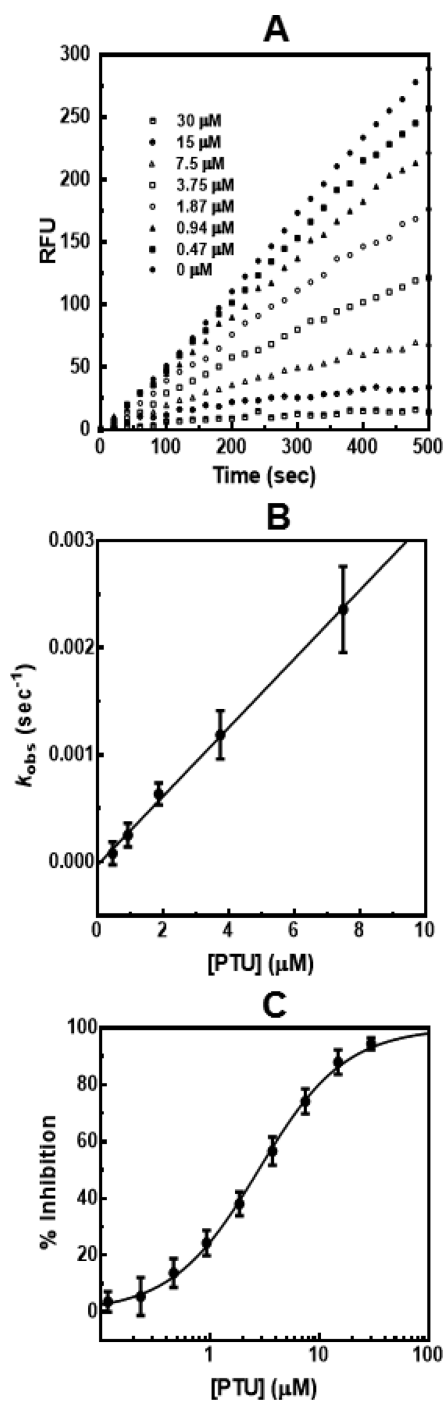


Figure 3. Inhibition of MPO by propylthiouracil. The MPO reactions were performed as described in Experimental Section. Data are averages, and error bars represent the SD from two separate experiments. (A) Progress curves for MPO inhibition by PTU varied at 0.47–30 μM. The k_{obs} values were obtained by fitting the time course as described in Experimental Section. (B) The k_{obs} values were fit to eq 3 to determine the overall potency k_{inact}/K_I ratio. (C) The initial rates from the first linear ~300 s of each reaction progress curve in (A) were used to calculate percent inhibition. The data were fit to equation, $y = 100/[1 + (x/IC_{50})^z]$, where IC₅₀ is the inhibitor concentration at 50% inhibition and z is the Hill slope.

activated inhibitory species proceeded to form a covalently inactivated MPO–PTU adduct only one time for every 76 turnover events of the MPO reaction with PTU. To determine the partition ratio, the percentage of control activity after rapid

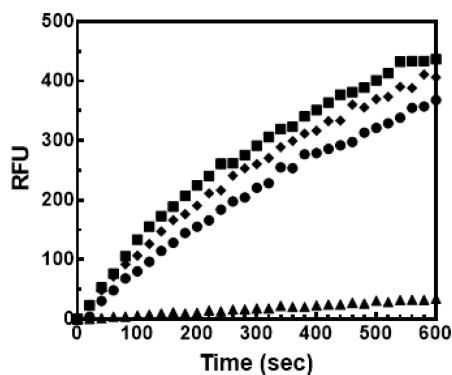


Figure 4. Reversibility of MPO inhibition by PTU. MPO was incubated with 24 μM PTU with (\blacktriangle) or without (\bullet) 2 μM H_2O_2 , or DMSO for control with (\blacksquare) or without (\blacklozenge) 2 μM H_2O_2 . After 15 min, an aliquot of the preincubation mixture was rapidly diluted 300-fold into the MPO reaction buffer containing 2 μM H_2O_2 and 30 μM Amplex Red substrates and the MPO activity was immediately monitored.

dilution was plotted as a function of the ratio of PTU versus MPO ($[\text{PTU}]/[\text{MPO}]$). As shown in Figure 5, the remaining

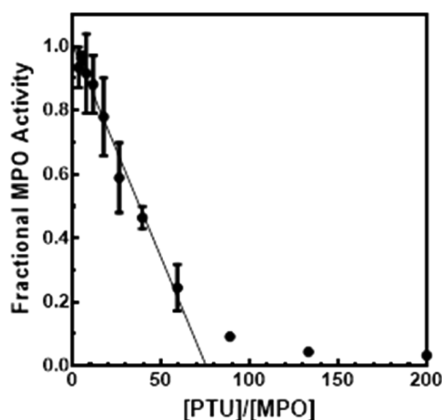


Figure 5. Determination of the partition ratio for mechanism-based inactivation of MPO by PTU. MPO was incubated with 2 μM H_2O_2 and PTU at concentrations varying by 1.5-fold between 0.026 and 12 μM (or DMSO for control). After 15 min, an aliquot of the preincubation mixture was rapidly diluted 300-fold into the assay buffer containing 2 μM H_2O_2 and 30 μM Amplex Red substrates and the MPO activity was immediately monitored. The initial rate of each progress curve was determined, and the fractional MPO activity of each inhibited reaction was plotted as a function of the ratio of PTU to MPO ($[\text{PTU}]/[\text{MPO}]$). Data are averages, and error bars represent the SD from two separate experiments.

fractional activity decreased as a linear function of $[\text{PTU}]/[\text{MPO}]$ until there was no activity remaining. The point at which this straight line intersected the x -axis was determined to be 76, which is equal to the partition ratio plus 1. For SAR purposes, the assay to determine partition ratios provided a measure of progress in the design of more efficient inhibitors (lower partition ratio). Higher efficiency inactivation was expected to be advantageous for in vivo efficacy and for safety (by minimizing the frequency of reactive intermediates escaping the MPO active site).

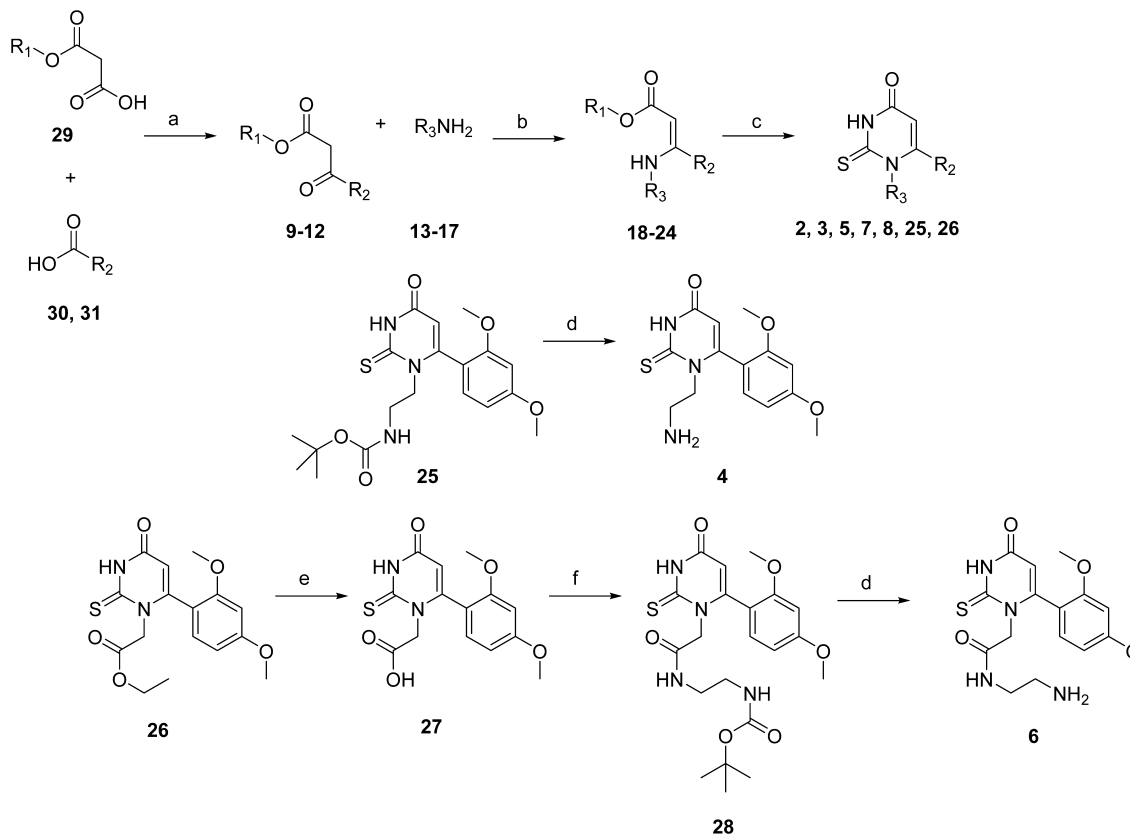
Concurrent with evaluation of compound potency utilizing biochemical assays, inhibition of MPO in a cell-based assay employing human whole blood stimulated with bacterial

lipopolysaccharide was also assessed.³⁹ The human whole blood assay provided a time-averaged inhibition of enzyme activity in the presence of potentially confounding factors (e.g., blood-borne electron donors, plasma protein binding, compartmental partitioning). While it remains to be established, it was assumed that the IC_{50} values obtained in human whole blood would correlate with the relative efficacious plasma concentrations in humans. Also uncertain at the outset was how well the human MPO biochemical assay ($k_{\text{inact}}/K_{\text{I}}$ ratio) would predict improvements in partition ratio or the human whole blood assay.

Chemistry. N1-Substituted-2-thiouracils have been previously synthesized via the condensation of appropriate mono-N-substituted-thiourea and β -ketoester derivatives to afford the corresponding N1- and N3-substituted-thiouracils as a mixture of regioisomers.⁴⁰ In the present work, the synthesis of the targeted N1-substituted-6-aryl-2-thiouracils was achieved by employing a regioselective two-step route (Scheme 1) involving the condensation of the appropriate β -ketoester intermediates (9–12) with the requisite primary amines (13–17) to yield the corresponding β -aminoacrylates (18–24). The β -ketoesters 11 and 12 were obtained via the reaction of ethyl hydrogen malonate (29) and the appropriate benzoic acid derivatives (intermediates 30 and 31) in the presence of magnesium ethoxide and 1,1'-carbonyldiimidazole. The corresponding N1-substituted-thiouracil analogs (2, 3, 5, 7, 8, 25, and 26) were thus obtained in a regiospecific manner by treatment of the β -aminoacrylates with isothiocyanatotrimethylsilane.⁴¹ Amine-containing side chain analogs were obtained by postcyclization modifications. Hydrochloric acid-catalyzed cleavage of the *tert*-butyloxycarbonyl protecting group in thiouracil 25 yielded 4 as the hydrochloride salt. Alternatively, hydrolysis of the thiouracil ester 26 yielded the carboxylic acid 27, which was then transformed to 28 by amide coupling with *tert*-butyloxycarbonyl ethylenediamine. Acid-catalyzed cleavage of the *tert*-butyloxycarbonyl protecting group in 28 generated amine 6 as the corresponding hydrochloride salt.

SAR Studies. Having established assays for the characterization of PTU inhibition of MPO and TPO, we utilized this compound as our starting point to seek thiouracil-based inhibitors with increased selectivity for MPO and decreased partition ratio. Initial SAR studies focused on replacement of the C6-propyl group and on introduction of an N1-substituent. Concurrently, considerations of the thiourea substructure contained within the thiouracil (see below) also led to a focus on a narrowly constrained target physicochemical properties space (roughly $\log D < 1.5$ to minimize CYP oxidative metabolism and nonproductive reactive metabolite formation while keeping $\text{PSA} < 100$ to maintain favorable membrane permeability and oral absorption) and the incorporation of specific polar functional groups in the N1-substituent.

In the course of our present SAR studies (Table 1), it was observed that replacement of the propyl group in PTU with an electron-rich aromatic functionality, such as the 2-methoxyphenyl group in 1, improved $k_{\text{inact}}/K_{\text{I}}$ ratio by 6-fold for MPO inhibition, although with only a modest improvement in inhibitory selectivity for MPO relative to TPO. However, far greater improvements in selectivity were obtained (>3000-fold) by substitution of the N1-position on the thiouracil ring, as shown in 2, which nearly abolished TPO inhibitory activity ($k_{\text{inact}}/K_{\text{I}} < 3 \text{ M}^{-1} \text{ s}^{-1}$, $\text{IC}_{50} > 100 \mu\text{M}$) while significantly increasing MPO $k_{\text{inact}}/K_{\text{I}}$ ratio by 21-fold from PTU.

Scheme 1. Synthesis of N1-Substituted-6-arylthiouracil Derivatives Described in This Study^a

^aReagents and conditions: (a) Mg ethoxide, CDI; (b) AcOH, 80 °C; (c) TMSNCS; (d) HCl; (e) NaOH; (f) NH₂CH₂CH₂NHBoc, T3P.

While these initial improvements in MPO inhibitory potency leading from PTU to **1** and **2** were observed employing the biochemical assay, similar improvements were not seen in the human whole blood assay (Table 1). Ongoing optimization of the N1- and C6-substituents showed that both made significant contributions to potency, and the combination ultimately led to compounds with improved whole blood potency. The preferred C6-ring system was found to be disubstituted phenyl, with the second substituent (methoxy or chloro) at the para (e.g., **2-6**) or meta (e.g., **7** and **8**) positions, providing a significant increase in potency; we concluded that MPO inhibitory potency was more dependent on the electron-density and substitution pattern on the C6-phenyl ring than on its overall hydrophobicity. Significant reductions in whole blood IC₅₀ were not afforded until $k_{\text{inact}}/K_{\text{I}}$ values were increased to $>10\,000\text{ M}^{-1}\text{ s}^{-1}$, although improvements in $k_{\text{inact}}/K_{\text{I}}$ values did not then strictly correlate with lower IC₅₀ values in the human whole blood assay (e.g., alcohol **3** vs amine **4**). Factors diminishing the direct correlation of potencies between the biochemical and whole blood assays may include differences in the unbound plasma concentrations (Table 2), distribution between compartments within whole blood, and/or varying contributions of the nonproductive single electron transfer (compound **II**) pathway in the biochemical assay. As such, potency improvement in the whole blood assay below $0.5\ \mu\text{M}$ proved to be highly challenging, especially while operating within a constrained physicochemical property space (see below for additional discussion). This may be due to modest affinity of the inhibitor for the active site (as reflected by the $>100\ \text{nM}$ K_{I} values from the Amplex Red assay), competition with high

concentration of native endogenous substrates (e.g., chloride and H₂O₂), dynamics of MPO activation in the assay, and/or efficiency of capture by the activated inhibitor species (partition ratio).

Concurrent with the development of SAR around substituents on the thiouracil ring, we initiated planning and experiments to better understand the risks associated with the thiouracil functionality. The thiouracil motif is considered a “structural alert” (analogous to the thiourea functionality) because of its propensity toward bioactivation to reactive species.⁴² For example, cases of immune-mediated hepatotoxicity and agranulocytosis have been reported in patients receiving chronic PTU treatment.^{43–45} There is causal evidence linking the immune-mediated toxicity to the oxidative bioactivation of PTU by MPO.^{34–37} In activated human polymorphonuclear leukocytes and/or human MPO/H₂O₂/Cl[−], PTU undergoes oxidative metabolism on its thiocarbonyl motif (Scheme 2) to yield PTU-disulfide, PTU-SO₂[−], and the protein- and thiol-reactive PTU-SO₃[−] as metabolites. It has been proposed that modification of neutrophil proteins, including MPO, may induce the formation of the antineutrophil antibodies that have been detected in patients with PTU-induced agranulocytosis^{46–48} and lupus-like syndrome.⁴⁹ In our present studies, liquid chromatography–tandem mass spectrometry (LC–MS/MS) analysis of an incubation of arylthiouracil **2** (exact mass (MH⁺) of 351.1367) with human MPO/H₂O₂/Cl[−] in the presence of excess glutathione (GSH) (1 mM) indicated the formation of a GSH conjugate (MH⁺ = 624.2334), which can be obtained via oxidation of the thiocarbonyl group in **2** to the putative sulfonate species

Table 1. Representative Set of in Vitro Pharmacology Data for N1-Substituted-6-arylthiouracil Analogs

Compd	R ₁	R ₂	logD ^a	MPO ^b			TPO ^b	Partition Ratio ^c	Human whole blood ^d
				pK _i (M)	p <i>k</i> _{inact} (s ⁻¹)	log(<i>k</i> _{inact} / <i>K</i> _i) (M ⁻¹ s ⁻¹)	log(<i>k</i> _{inact} / <i>K</i> _i) (M ⁻¹ s ⁻¹)		MPO IC ₅₀ (μM)
PTU	-(CH ₂) ₂ CH ₃	-H	0.85			2.56 ± 0.09	2.65 ± 0.02	75	5.7 [2.0 – 16]
1		-H	1.3			3.36 ± 0.25	2.86 ± 0.10		6.2 [4.0 – 9.5]
2			2.6	6.30 ± 0.15	2.43 ± 0.04	3.87 ± 0.12	< 0.5		11 [6.6 – 17]
3			1.1	6.82 ± 0.01	2.34 ± 0.01	4.47 ± 0.01	< 0.5	10	2.0 [1.4 – 2.7]
4			-0.17	6.76 ± 0.09	2.61 ± 0.03	4.13 ± 0.08	< 0.5	4.7	0.50 [0.38 – 0.68]
5			0.59	6.43 ± 0.05	2.41 ± 0.03	4.03 ± 0.05	< 0.5	15	2.6 [2.0 – 3.4]
6			-1.4			4.03 ± 0.08	< 0.5		0.60 [0.48 – 0.75]
7			0.34	6.46 ± 0.09	2.38 ± 0.05	4.09 ± 0.06	< 0.5		1.5 [1.3 – 1.7]
8			0.81	6.50 ± 0.14	2.43 ± 0.08	4.07 ± 0.09	< 0.5	6.5	1.9 [1.7 – 2.2]

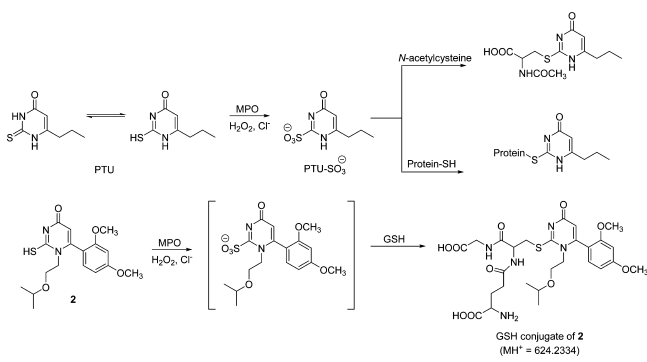
^alog *D* was measured at pH 7.4 using the previously described shake-flask method.⁵⁵ ^b*k*_{inact} and *K*_i values were determined as described in Experimental Section. Values are the geometric mean [90% CI] of at least two independent experiments. The overall potency (*k*_{inact}/*K*_i) was calculated using these mean values. When *k*_{inact} and *K*_i values could not be determined separately (i.e., *K*_i ≫ [I]), the *k*_{inact}/*K*_i ratios were obtained from the slopes, similar to Figure 3B, and values listed are the geometric mean values (±90% CI) of at least two independent experiments. The *k*_{inact}/*K*_i ratios given for TPO inhibition are geometric mean values [90% CI] that when measurable were obtained by using initial rates from the first 300 s of the reaction at each inhibitor concentration. ^cPartition ratios were generated from two to four separate experiments. ^dIC₅₀ values shown are geometric mean values [90% CI] of individual determinations for inhibition of MPO activity in LPS-stimulated human whole blood.

Table 2. Representative in Vitro ADME Data for N1-Substituted-6-arylthiouracil Analogs

compd	PSA (\AA^2)	permeability RRCK P_{app} (10^{-6} cm/s) ^a	human PPB f_u ^b	HLM $CL_{\text{int,app}}$ ($\mu\text{L min}^{-1} \text{mg}^{-1}$) ^c	HHEP $CL_{\text{int,app}}$ ($\mu\text{L min}^{-1}$ per 10^6 cells) ^c
2	65	26	ND ^d	11	ND ^d
3	76	13	0.5	<8.0	<6.0
4	82	3.5	0.7	8.8	2.9
5	99	0.8	0.5	<8.0	<6.0
6	111	1.5	0.9	<8.0	<6.0
7	99	1.1	0.6	<8.0	<6.0
8	90	1.6	0.4	<8.0	<6.0

^aPassive permeability was determined in Ralph–Russ canine kidney cells, which are a low transporter cell line, isolated from Madine–Darby canine kidney cells.⁵⁷ ^bFraction unbound (f_u) in human plasma was determined from equilibrium dialysis method and is a mean value from three individual determinations.⁵⁸ ^c $CL_{\text{int,app}}$ refers to total apparent intrinsic clearance obtained from scaling in vitro half-lives in HLM and HHEP as previously described.⁶³ ^dND = not determined.

Scheme 2. Oxidative Bioactivation of the Thiouracil Motif in PTU and Compound 2



followed by nucleophilic displacement in the presence of exogenously added GSH (Scheme 2).

With awareness of the high partition ratio of PTU, we speculated that systemic exposure to reactive species derived from oxidative bioactivation of the thiocarbonyl motif (e.g., the corresponding sulfonate) could be minimized if a pendent nucleophilic group were tethered to the N1-substituent such that potential thiocarbonyl reactive species in solution could be rapidly quenched in an intramolecular fashion. At the outset it

was not obvious whether such a tactic would compromise the ability of the compound(s) to inhibit MPO in the desired irreversible and selective manner. However, optimization of the N1-substituent demonstrated that small polar groups such as a hydroxyl (3), amino (4), or amidoyl (5) not only were tolerated for MPO inhibition but also enhanced the effectiveness of the arylthiouracil to act as an irreversible inhibitor, as evidenced by their increased k_{inact}/K_I and their lower IC_{50} in the human whole blood assay (Table 1). Higher potencies in the biochemical assay were observed with alcohols (e.g., 3, $k_{\text{inact}}/K_I = 29\,800$), while greater inhibitory potencies in the human whole blood assay were obtained with the amines (e.g., 4 and 6, human whole blood IC_{50} of 0.50 and 0.60 μM , respectively). Although not as robust an MPO potency improvement when compared with the alcohol and amine variants, the primary carboxamide functionality (e.g., 5) also provided another viable alternative for modulating physical properties in the balance of efficacy and safety. Gratifyingly, compounds 3–5 also displayed a greatly improved MPO inactivation efficiency (partition ratio) with 4 possessing the highest inactivation efficiency (lowest partition ratio) of 4.7 (versus 75 for PTU), which suggested that MPO inactivation efficiency may be a key determinant of inhibitory activity in the human whole blood assay.

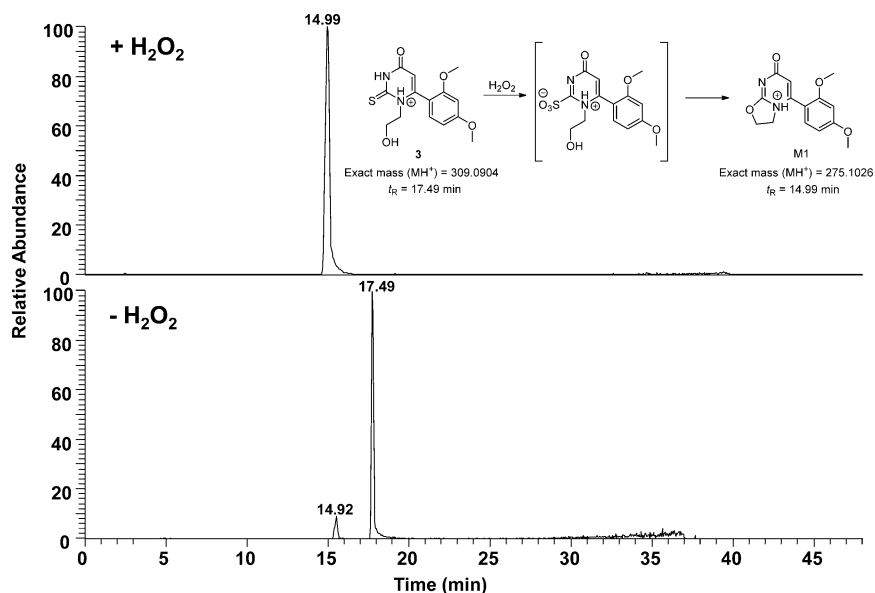


Figure 6. LC–MS/MS analysis of the oxidative metabolism of alcohol 4 to cyclic ether M1 in the presence of H_2O_2 .

Table 3. Preclinical Pharmacokinetics^a of Selected N1-Substituted-6-arylthiouracil Derivatives

compd	species	CL _p (mL min ⁻¹ kg ⁻¹)	V _{ds} (L/kg)	t _{1/2} (h)	T _{max} (h) ^b	oral F (%) ^b
3	rat	59.3 ± 2.65	0.82 ± 0.02	0.25 ± 0.01	1.3 ± 0.6	8
	dog	11.9 ± 2.87	1.33 ± 0.26	5.3 ± 0.7	1.17 ± 0.76	16
4	rat	70.3 (79, 69.5)	3.71 (4.34, 3.08)	1.1 (0.9, 1.2)	0.38 (0.25, 0.50)	91
	dog	13.4 (12.3, 14.4)	3.66 (3.89, 3.43)	5.7 (5.8, 5.7)	1.3 (2.0, 0.5)	84
5	rat	35.1 (35.8, 34.4)	1.23 (1.37, 1.09)	0.76 (1.02, 0.50)	0.5 (0.5, 0.5)	76
	dog	1.31 (1.44, 1.17)	0.30 (0.29, 0.30)	3.4 (3.2, 3.6)	1.5 (2.0, 1.0)	31
6	rat	38.6 ± 5.52	0.59 ± 0.17	0.81 ± 0.02	0.75 (0.5, 1.0)	3
	dog	4.10 (3.81, 4.39)	0.86 (0.74, 0.97)	2.59 (2.50, 2.68)	1.0 (1.0, 1.0)	8
7	rat	37.6 ± 1.36	0.83 ± 0.16	0.38 ± 0.19	0.67 ± 0.29	61
	dog	7.07 (7.86, 6.27)	1.03 (0.92, 1.14)	2.80 (1.70, 3.90)	0.63 (1.0, 0.25)	100
8	rat	41.8 ± 9.65	2.13 ± 1.08	0.75 ± 0.19	0.78 ± 1.10	86
	mouse	10.1 ± 0.83	0.90 ± 0.06	1.36 ± 0.12	1.0 ± 0.1	100
	dog	3.39 ± 1.13	0.54 ± 0.04	2.2 ± 0.5	0.7 ± 0.3	75
	monkey	10.3 (10.5, 10.1)	1.09 (1.17, 1.01)	3.28 (3.31, 3.24)	1.5 (1.0, 2.0)	76

^aAll experiments involving animals were conducted in our AAALAC-accredited facilities and were reviewed and approved by Pfizer Institutional Animal Care and Use Committee. Pharmacokinetic parameters were calculated from plasma concentration–time data and are reported as mean values (±SD for $n = 3$ and individual values for $n = 2$). All pharmacokinetics were conducted in male gender of each species (Wistar rats, CD-1 mice, beagle dogs, and/or cynomolgus monkey). Intravenous (iv) doses for the test compounds were 1 mg/kg, and compounds were administered in saline (compounds 4 and 6) or 12% sulfobutyl ether β -cyclodextrin (compounds 3, 4, 5, 7, and 8) solution. Oral (po) doses for the test compounds were either 3 or 5 mg/kg, and compounds were formulated in 0.5% methylcellulose. ^bObtained from po dose.

Oxidative desulfurization of thioureas to ureas by H₂O₂ is a well-studied reaction.^{50,51} Therefore, an initial assessment of the viability of the intramolecular trapping of reactive species with the pendent nucleophile was conducted via reacting alcohol 3 (10 μ M) with H₂O₂ (500 μ M) in phosphate buffer (pH 7.4) for 60 min at 37 °C. While no sulfonic acid metabolite could be observed, its presence as an intermediate in the incubation was inferred from the quantitative conversion of 3 ($t_R = 17.49$ min, MH⁺ = 309.0903) to the stable cyclic ether M1 ($t_R = 14.99$ min, MH⁺ = 275.1026) as a metabolite (Figure 6) upon analysis by LC–MS/MS. The formation of M1 was also noted in incubations of 3 (10 μ M) in the MPO/H₂O₂/Cl⁻ system in a H₂O₂-dependent fashion, although the reaction was not quantitative likely due to rapid inhibition of MPO activity. Importantly, no sulfhydryl conjugates of 3 were detected upon addition of excess GSH (1 mM) to the H₂O₂ or MPO/H₂O₂/Cl⁻ incubations. A similar analysis with thiouracils 4, 6, 7, and 8 in the MPO/H₂O₂/Cl⁻ system in the presence of excess GSH also failed to generate GSH adducts. Overall, these observations support the hypothesis that although an undesired reactive metabolite may be formed in the course of MPO catalysis, the intramolecular trapping mechanism provides the potential for decreasing exposure to the reactive metabolite(s) in vivo.

Besides peroxidases, heme-containing CYPs or other oxidative enzymes such as flavin monooxygenases in human hepatic tissues (e.g., human liver microsomes (HLM) and cryopreserved hepatocytes (HHEP)) are also capable of oxidizing the thiourea/thiouracil functionalities to reactive species capable of eliciting a toxicological response.^{42,52–54} In the present situation, minimization of oxidative metabolism/bioactivation of the thiouracil derivatives was largely driven through a reduction in lipophilicity as determined by log $D_{7.4}$.^{55,56} Aiding in this endeavor was an only modest dependency between log D and MPO inhibitory potency as noted earlier. Virtually all compounds prepared with log $D < 1.5$ were resistant to metabolic turnover in prototypic stability studies in NADPH-supplemented HLM and HHEP, as reflected from their very low apparent intrinsic clearance (CL_{int,app}) values (Table 2). However, while potency and

metabolic clearance tended to favor molecules at the lower ranges of hydrophobicity, the less-lipophilic analogs obtained with increasingly polar functionalities (e.g., *N*-ethylaminoamide 6, PSA = 111) showed impairment in passive membrane permeability (P_{app}) as measured in the Ralph–Russ canine kidney (RRCK) assay⁵⁷ (Tables 1 and 2). Fortunately, the range of physicochemical properties discovered to be tolerated within this series of thiouracils provided sufficient latitude to allow overall balance to be achieved with regard to absorption, distribution, metabolism, and excretion (ADME) properties discussed below.

Pharmacokinetics and in Vitro ADME Profiling. A subset of *N*1-substituted-6-arylthiouracils that met the MPO inhibitory potency and selectivity criteria were advanced to intravenous (iv) and po pharmacokinetic studies in preclinical species. The pharmacokinetic parameters describing the disposition are summarized in Table 3. Following iv administration to rats, compounds 5–7 demonstrated moderate plasma clearance (CL_p) ranging from 35.1 to 38.6 mL min⁻¹ kg⁻¹, while compounds 3 and 4 exhibited high CL_p (59–70 mL min⁻¹ kg⁻¹), which approached the rat hepatic blood flow of 70–80 mL min⁻¹ kg⁻¹. In contrast, compounds 3–7 exhibited relatively low CL_p (1.31–13.4 mL min⁻¹ kg⁻¹) in dogs. Furthermore, with the exception of primary alcohol 3 and basic amine 6, good oral bioavailability (F) was discerned with 4, 5, and 7 in rats and dogs (oral F of 3 and 6 was 8.0–16% in rats and dogs; oral F of 4, 5, and 7 was 31–100% in rats and dogs).

In the course of balancing MPO inhibitory potency, TPO selectivity, and in vivo pharmacokinetics, our focus was drawn to the series of acetamides (compounds 6, 7, and 8). At the lower end of the lipophilicity range, *N*-ethylaminoamide 6 demonstrated potent inhibition of MPO activity (IC₅₀ = 0.6 μ M) in human whole blood. However, clinical viability of 6 was limited due to its low oral systemic bioavailability in preclinical species, which may be a consequence of its low membrane permeability due to its high polarity and PSA (log $D_{7.4} = -1.4$, PSA = 111). Each member of the pair of primary amides possessing a pendent 2,5-disubstituted phenyl group (com-

pounds 7 and 8) was considered for further investigations due to their improved MPO inhibitory potency relative to 5, as well as the observed high oral bioavailability (Table 3). While both compounds possessed desirable attributes, 8 was advanced into a preclinical pharmacology study in non-human primates due to advantages in thermodynamic solubility and predicted human bioavailability.

The in vivo pharmacokinetics of 8 were examined in greater detail in mice, rats, dogs, and monkeys, wherein it was demonstrated to have low CL_p in mice ($10.1 \text{ mL min}^{-1} \text{ kg}^{-1}$), dogs ($3.39 \text{ mL min}^{-1} \text{ kg}^{-1}$), monkeys ($10.3 \text{ mL min}^{-1} \text{ kg}^{-1}$) and moderate CL_p in rats ($41.8 \text{ mL min}^{-1} \text{ kg}^{-1}$). The terminal plasma elimination half-lives ($t_{1/2}$) ranged from 0.75 to 3.3 h in the four species. Approximately 26–32% of the iv dose of 8 was excreted in the unchanged form in rat, dog, and monkey urine, wherein it was also shown that it was well distributed with steady state distribution volumes (V_{dss}) ranging from 0.5–2.1 L/kg in mice, rats, dogs, and monkeys. Following oral administration, 8 was rapidly ($T_{max} = 0.78\text{--}1.70 \text{ h}$) and well absorbed in mice, rats, dogs, and monkeys with oral bioavailability values of 100%, 86%, 75%, and 76%, respectively. The mean plasma free fraction (f_u) of 8 ($2 \mu\text{M}$), determined by equilibrium dialysis,⁵⁸ in mouse, rat, dog, monkey, and human was 0.451, 0.447, 0.460, 0.536, and 0.376, respectively. The ability of 8 to reversibly inhibit the major human CYP enzymes was investigated in human liver microsomes using established protocols.⁵⁹ Likewise, the potential of 8 to inhibit major human CYP enzymes in a time- and concentration-dependent manner was assessed using an IC_{50} shift assay in human liver microsomes.⁶⁰ In addition, 8 demonstrated no reversible inhibition and no change in time-dependent inhibitory potency ($IC_{50} > 100 \mu\text{M}$) against CYP1A2, CYP2B6, CYP2C8, CYP2C9, CYP2C19, CYP2D6, and CYP3A4 catalytic activities in human liver microsomes. Consistent with its low lipophilicity ($\log D_{7.4} = 0.81$), 8 was resistant toward metabolic turnover in NADPH-supplemented HLM and cryopreserved HHEP and was devoid of GSH adduct formation in these biochemical matrices. On the basis of these observations and physicochemical properties (including low $\log D$ and low passive permeability), we speculate that metabolic elimination will be inconsequential as a clearance mechanism in humans and that 8 will be principally eliminated via renal excretion in the unchanged form.⁶¹ In addition, 8 was also devoid of mutagenic responses in the *Salmonella* Ames and in vitro micronucleus assays in the absence or presence of CYP activation (aroclor-induced rat liver S9 fraction/NADPH), and no significant off-target activity was discerned upon evaluation of 8 (at $100 \mu\text{M}$) across a broad panel of receptors, ion channels, enzymes, and transporters.

In Vivo Pharmacology. In order to ascertain whether the advances noted in the in vitro and ex vivo assays for candidate thioracil derivatives translated to effective irreversible inhibition of MPO in vivo, 8 was also advanced to an in vivo pharmacology study in cynomolgus monkeys using iv endotoxin (LPS) challenge, a classic model of inflammatory leukocyte activation with corresponding MPO activation demonstrated in various species including human.⁶² In this randomized crossover study, cynomolgus monkeys were orally administered either vehicle or 8 (5, 20, and 80 mg/kg) 1 h after iv administration of LPS. Blood was sampled throughout the study and heparinized plasma prepared for MPO activity measurements as well as determination of 8 plasma concentrations. Total MPO was captured using anti-MPO

antibody coated plates, and following exchange of plasma for drug-free assay media, the residual activity of the captured MPO was measured using the peroxidation of Amplex Red. A mixed effect sigmoid model was applied to study the relationship between plasma exposure of 8 and the MPO capture activity at 2 h after dose and 3 h after LPS administration, which corresponds to the peak of MPO activity. As shown in Figure 7, the estimated EC_{50} for total 8 concentration in plasma was $3.8 \mu\text{M}$, which corresponds well with the IC_{50} value obtained in the human whole blood assay of $1.9 \mu\text{M}$.

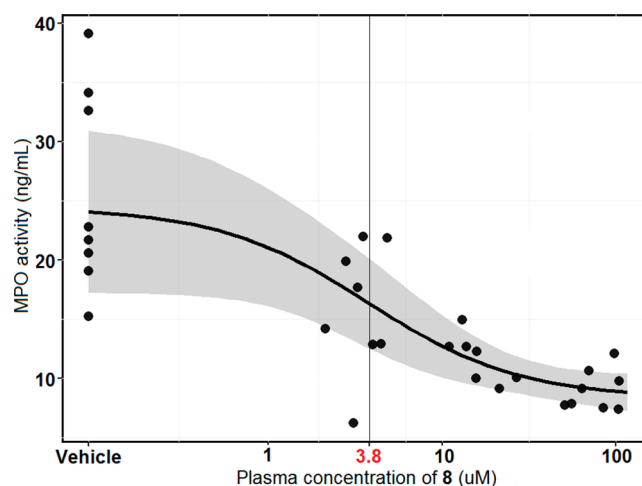


Figure 7. Concentration–effect relationship for inhibition of MPO activity by 8 in a cynomolgous monkey LPS challenge study. Compound 8 was administered orally (5, 20, and 80 mg/kg) 1 h after iv administration of LPS. After 2 h (the peak in MPO activity) plasma samples were collected and concentrations of 8 as well as residual MPO activity determined. The plasma concentration of 8 that correlated with 50% of the maximum MPO inhibition achieved was $3.8 \mu\text{M}$, approximately twice the IC_{50} observed in the human whole blood assay ($1.9 \mu\text{M}$).

Summary. We have described the design, synthesis, and preclinical evaluation of N1-substituted-6-aryl-2-thiouracils as potent mechanism-based inactivators of MPO with great improvements in MPO inactivation efficiency (as evidenced by reduced partition ratio) over PTU. Furthermore, in contrast with PTU, the N1-substituted-6-aryl-2-thiouracil derivatives also demonstrated high selectivity over the related haloperoxidase TPO. Upon the basis of its potent and selective MPO inhibitory characteristics, lack of oxidative metabolism in HLM and HHEP, clean off-target profile including lack of measurable TPO activity, as well as favorable preclinical in vivo safety results, PF-06282999 (8) has been advanced to clinical trials for human pharmacokinetics, safety/tolerability, and MPO inhibition studies, which are currently underway and will be reported in due course.

EXPERIMENTAL SECTION

MPO Assay and Determination of Inhibitor Potency (k_{inact}/K_i Ratios). MPO was purified from human polynuclear leukocytes, and MPO peroxidase activity was measured by monitoring the formation of resorufin generated from the oxidation of Amplex Red by MPO as described previously.³¹ Briefly, the assay mixture contained 50 mM sodium phosphate buffer, pH 7.4, 150 mM NaCl, 1 mM diethylenetriaminepentaacetic acid, $2 \mu\text{M H}_2\text{O}_2$, $30 \mu\text{M}$ Amplex Red, and the indicated concentrations of inhibitor (or DMSO). Reactions were

initiated by the addition of 100 pM MPO, and the final concentration of DMSO was kept at 2%. The first ~600 s of the reaction progress curves corresponding to the linear range of the DMSO control were fit to eq 1.

$$\text{product} = \frac{V_0}{k_{\text{obs}}} [1 - \exp(-k_{\text{obs}}t)] \quad (1)$$

where V_0 is the initial rate in RFU/s and t is time in seconds, to obtain the first order rate constant for enzyme inactivation (k_{obs}) at each inhibitor concentration. Each k_{obs} value was corrected for auto-inactivation of the enzyme by subtracting the k_{obs} value for the uninhibited reaction. The corrected k_{obs} values were then plotted versus inhibitor concentration ($[I]$) and fit to eq 2.

$$k_{\text{obs}} = \frac{k_{\text{inact}}[I]}{K_1 + [I]} \quad (2)$$

where k_{inact} is the maximal rate of inactivation and K_1 is the inhibitor concentration that yields half the rate of maximal inactivation. When $[I] \ll K_1$, eq 2 is simplified to eq 3,

$$k_{\text{obs}} = \frac{k_{\text{inact}}}{K_1} [I] \quad (3)$$

where the k_{inact}/K_1 is calculated from the slope, which is obtained from the k_{obs} vs $[I]$ linear lines.³⁸ All assays were performed in 96-well, black, half-area, nonbinding surface, polystyrene plates (Corning, Tewksbury, MA). Fluorescent changes (relative fluorescent units/s, RFU/s) were monitored at room temperature every 20 s on a Spectramax M2 microplate spectrophotometer (Molecular Devices, Palo Alto, CA) equipped with Softmax Pro software (Molecular Devices, Palo Alto, CA) with excitation and emission filters set at 530 and 580 nm, respectively. All data were analyzed using nonlinear regression analysis in Microsoft Excel and Kaleidagraph (Synergy Software, Reading, PA).

TPO Assay. TPO activity was measured by monitoring the formation of resorufin from the oxidation of Amplex Red using conditions similar to those in the described in the MPO assay.³⁹ Assay mixtures (100 μ L) contained 50 mM sodium phosphate buffer, pH 7.4, 150 mM NaCl, 2 μ M H₂O₂, 30 μ M Amplex Red, 1 mM diethylenetriaminepentaacetic acid, and 2% DMSO. The reactions were initiated by the addition of TPO. Reaction mixtures to determine the background reaction rate consisted of all assay components and 4 μ L of 500 unit/mL bovine catalase in 50 mM potassium phosphate buffer, pH 7.0. The background rate was subtracted from each reaction progress curve. All data were analyzed using nonlinear regression analysis in Microsoft Excel and Kaleidagraph (version 3.5, Synergy Software).

Human Whole Blood Assay for Irreversible Inhibition of MPO. MPO activity was determined using modifications to a described method,⁶² using human whole blood from healthy volunteers, collected in heparinized tubes. Test compound was incubated with human whole blood stimulated with bacterial LPS for 4 h, followed by capture of MPO on immobilized anti-MPO antibody coated plates. The captured MPO was washed and residual MPO activity was determined using Amplex Red and H₂O₂ as described in our previous publication.³⁹

Compound Synthesis. All chemicals, reagents, and solvents were purchased from commercial sources and were used without further purification. Except where otherwise noted, all reactions were run under an inert atmosphere of nitrogen gas using anhydrous solvents. Also, except where otherwise noted, all reactions were run at room temperature (~23 °C). The term "concentrated" refers to the removal of solvent at reduced pressure on a rotary evaporator with a water bath temperature not exceeding 60 °C. Silica gel chromatography was performed using a medium pressure Biotage or ISCO system and columns prepackaged by various commercial vendors including Biotage and ISCO. PTU and 6-(2-methoxyphenyl)-2-thioxo-2,3-dihydropyrimidin-4(1H)-one (**1**) were purchased from commercial sources. Compound **7** (also known as PF-1355 or PF-06281355) is commercially available from Sigma-Aldrich (catalog no. PZ0277).

NMR spectra were recorded on 400 or 500 MHz spectrometers and are reported relative to residual undeuterated solvent signals. Data for ¹H NMR spectra are reported as follows: chemical shift (δ), multiplicity, coupling constant (Hz), and integration. The peak shapes are denoted as follows: s, singlet; d, doublet; dd, doublet of doublets; t, triplet; q, quartet; spt, septet; m, multiplet; br s, broad singlet. Mass spectrometry (MS) was performed via atmospheric pressure chemical ionization (APCI) or electron scatter (ES) ionization sources. High-resolution mass spectrometry (HRMS) was performed via electrospray ionization (ESI) source. The system used was an Agilent 1200 DAD (G1315C), 190–400 nm scan, 4 nm slit, and Agilent 6220 MS (TOF). Where the intensity of single chlorine ions is described, the expected intensity ratio was observed (approximately 3:1 for ³⁵Cl/³⁷Cl-containing ions) and the intensity of only the lower mass ion is given. Elemental analyses were performed by Intertek Pharmaceutical Services, Whitehouse, NJ. HPLC purity was determined using a Kinetex C18 column (100 mm \times 3.0 mm, 2.6 μ m), eluting with 95:5 water/acetonitrile (both solvents containing 0.1% formic acid), flow rate = 0.75 mL/min, detecting at 215 nm. HPLC purity is reported as >95% if no peaks other than the desired product were observed.

Ethyl (Z)-3-(2,4-Dimethoxyphenyl)-3-((2-isopropoxyethyl)-amino)acrylate (18**).** A solution of ethyl 3-(2,4-dimethoxyphenyl)-3-oxopropanoate (**9**) (0.95 g, 4.0 mmol) and 2-isopropoxyethan-1-amine (**13**) (1.3 g, 12.0 mmol) in ethanol (4 mL) was treated with acetic acid (0.70 mL, 12.0 mmol) and then heated at reflux. After 64 h, the reaction mixture was allowed to cool to ambient temperature and concentrated under reduced pressure. The resulting residue was dissolved in dichloromethane (400 mL) and washed sequentially with an aqueous 1 M HCl solution (100 mL), a saturated aqueous sodium bicarbonate solution (100 mL), and brine (100 mL). The organic layer was dried over MgSO₄ and concentrated. The resulting crude product was purified by flash column chromatography on silica gel using a gradient of 5–10% ethyl acetate in heptane to afford the title compound **18** (0.75 g, 56%). ¹H NMR (400 MHz, CDCl₃) δ 8.74 (t, J = 5.7 Hz, 1 H), 7.12 (d, J = 8.2 Hz, 1 H), 6.48 (dd, J = 8.2, 2.1 Hz, 1 H), 6.45 (d, J = 2.3 Hz, 1 H), 4.46 (s, 1 H), 4.13 (q, J = 7.0 Hz, 2 H), 3.82 (s, 3 H), 3.80 (s, 3 H), 3.55 (spt, J = 6.1 Hz, 1 H), 3.40 (t, J = 6.1 Hz, 2 H), 3.11 (m, 2 H), 1.26 (t, J = 7.1 Hz, 3 H), 1.14 (d, J = 6.3 Hz, 6 H). LCMS (ESI⁺) m/z : 338.2 [M + H]⁺ (100%).

6-(2,4-Dimethoxyphenyl)-1-(2-isopropoxyethyl)-2-thioxo-2,3-dihydropyrimidin-4(1H)-one (2**).** A mixture of ethyl (Z)-3-(2,4-dimethoxyphenyl)-3-((2-isopropoxyethyl)amino)acrylate (**18**) (0.64 g, 1.9 mmol) and isothiocyanatotrimethylsilane (1.1 mL, 9.4 mmol) was heated at 110 °C by microwave irradiation for 1 h. After cooling to ambient temperature, the reaction mixture was directly purified by flash column chromatography on silica gel, eluting with a 5–10% gradient of ethyl acetate in heptane to afford **2** (0.54 g, 80%) as a pale yellow solid. ¹H NMR (400 MHz, CDCl₃) δ 9.88 (br s, 1 H), 7.14 (d, J = 8.4 Hz, 1 H), 6.54 (dd, J = 8.4, 2.3 Hz, 1 H), 6.49 (d, J = 2.1 Hz, 1 H), 5.79 (s, 1 H), 4.63–4.71 (m, 1 H), 3.85 (s, 3 H), 3.81 (s, 3 H), 3.67–3.84 (m, 2 H), 3.48 (ddd, J = 9.8, 5.9, 3.1 Hz, 1 H), 3.45 (spt, J = 6.1 Hz, 1 H), 1.030 (d, J = 6.1 Hz, 3 H), 1.027 (d, J = 6.1 Hz, 3 H). LCMS (ESI⁺) m/z : 351.2 [M + H]⁺ (100%). HRMS: m/z calcd for C₁₇H₂₃N₂O₄S [M + H]⁺ 351.1379, found 351.1373. Anal. Calcd for C₁₇H₂₃N₂O₄S: C, 58.27; H, 6.33; N, 7.99; S, 9.15. Found: C, 57.81; H, 6.25; N, 7.81; S, 9.18. HPLC purity: >95%.

Methyl (Z)-3-(2,4-Dimethoxyphenyl)-3-((2-hydroxyethyl)-amino)acrylate (19**).** A mixture of methyl 3-(2,4-dimethoxyphenyl)-3-oxopropanoate (**10**) (3.50 g, 14.69 mmol) and acetic acid (0.17 mL, 2.94 mmol) in isopropanol (70 mL) was combined with ethanolamine (0.88 mL, 14.69 mmol) and heated to 80 °C. After 2, 4, and 6 h, additional ethanolamine (0.88 mL, 14.69 mmol) was added to the reaction mixture. After 48 h, the reaction mixture was cooled to ambient temperature and then concentrated under reduced pressure. The resulting residue was suspended in equal parts of a saturated sodium bicarbonate solution and water under N₂. After stirring overnight, the solids were filtered and dried in a vacuum oven at 30 °C overnight to afford **19** (2.72 g, 63%) as a beige colored powder. ¹H NMR (400 MHz, CDCl₃) δ 8.77 (t, J = 5.4 Hz, 1 H), 7.13 (d, J = 8.3 Hz, 1 H), 6.47–6.52 (m, 2 H), 4.53 (s, 1 H), 3.84 (s, 3 H), 3.82 (s, 3

H), 3.66 (s, 3H), 3.61 (td, $J = 5.5, 5.5$ Hz, 2 H), 3.15 (td, $J = 5.5, 5.5$ Hz, 2 H).

6-(2,4-Dimethoxyphenyl)-1-(2-hydroxyethyl)-2-thioxo-2,3-dihydropyrimidin-4(1H)-one (3). A solution of methyl (Z)-3-(2,4-dimethoxyphenyl)-3-((2-hydroxyethyl)amino)acrylate (**19**) (9.50 g, 33.8 mmol) in 2-methyltetrahydrofuran (100 mL) was treated with isothiocyanatotrimethylsilane (23.80 mL, 168.79 mmol), and the resulting reaction mixture was heated at 85 °C. After stirring overnight, the reaction mixture was cooled to ambient temperature, extracted with an aqueous 1 N NaOH solution (1 × 250 mL, then 1 × 50 mL); the combined aqueous layers were washed with methylene chloride (2 × 50 mL), and the aqueous phase was acidified to pH 4 with concentrated HCl. The resulting solids were collected by filtration, washed with water (2 × 50 mL), and dried under N₂ overnight to afford a light yellow powder. This material was then dissolved in DMF (70 mL) at 90 °C before water (80 mL) was added to the hot solution. After allowing this solution to cool to ambient temperature and stirring overnight, the resulting solids were filtered, washed with water, and dried under high vacuum to provide **3** (6.7 g, 61%) as an off-white powder. ¹H NMR (500 MHz, DMSO-*d*₆) δ 12.68 (s, 1 H), 7.24 (d, $J = 8.3$ Hz, 1 H), 6.69 (d, $J = 2.4$ Hz, 1 H), 6.65 (dd, $J = 8.4, 2.3$ Hz, 1 H), 5.70 (d, $J = 2.2$ Hz, 1 H), 4.69 (t, $J = 4.9$ Hz, 1 H), 4.50 (ddd, $J = 13.4, 7.1, 4.2$ Hz, 1 H), 3.83 (s, 3 H), 3.82 (s, 3 H), 3.59 (dt, $J = 13.4, 7.3$ Hz, 1 H), 3.46–3.55 (m, 1 H), 3.38–3.46 (m, 1 H). MS (ESI⁺) m/z : 309.1 [M + H]⁺. HRMS: m/z calcd for C₁₄H₁₇N₂O₄S [M + H]⁺ 309.0909, found 309.0906. Anal. Calcd for C₁₄H₁₆N₂O₄S: C, 54.53; H, 5.23; N, 9.09; S, 10.40. Found: C, 54.29; H, 5.14; N, 8.98; S, 10.43. HPLC purity: 98.1%.

Ethyl (Z)-3-(2-(tert-butoxycarbonylamino)ethylamino)-3-(2,4-dimethoxyphenyl)acrylate (20). A solution of ethyl 3-(2,4-dimethoxyphenyl)-3-oxopropanoate (**9**) (41.91 g, 166 mmol) and *tert*-butyl (2-aminoethyl)carbamate (**15**) (54.7 g, 342 mmol) in ethanol (180 mL) was treated with acetic acid (16.14 g, 269 mmol) and heated at reflux. After ~5 h, the reaction mixture was cooled to ambient temperature and concentrated under reduced pressure. The resulting residue was partitioned between ethyl acetate (300 mL) and a 10% (w/v) aqueous ammonium chloride solution. The organic layer was separated and washed with water, 10% (w/v) aq ammonium chloride (3 mL), and brine (10 mL). The organic layer was then agitated with a saturated aqueous sodium bicarbonate solution, to which brine (6 mL) was added, and the phases were separated. The organic layer was washed with brine and dried (Na₂SO₄). Concentration of the organic layer afforded **20** as a viscous, amber solid (62.3 g, 95%), which was used in the subsequent procedure without further purification. ¹H NMR (500 MHz, CDCl₃) δ 8.65 (br s, 1 H), 7.12 (d, $J = 8.3$ Hz, 1 H), 6.50 (dd, $J = 8.4, 1.8$ Hz, 1 H), 6.47 (d, $J = 1.7$ Hz, 1 H), 4.88 (br s, 1 H), 4.51 (s, 1 H), 4.14 (q, $J = 7.1$ Hz, 2 H), 3.83 (s, 6 H), 3.03–3.21 (m, 4 H), 1.43 (s, 9 H), 1.27 (t, $J = 7.1$ Hz, 3 H). LCMS (ESI⁺) m/z : 395.4 [M + H]⁺ (100%).

***tert*-Butyl 2-(6-(2,4-Dimethoxyphenyl)-4-oxo-2-thioxo-3,4-dihydropyrimidin-1(2H)-yl)ethylcarbamate (25).** A solution of ethyl (Z)-3-(2-(*tert*-butoxycarbonylamino)ethylamino)-3-(2,4-dimethoxyphenyl)acrylate (**20**) (62.3 g, 158 mmol) in 2-methyltetrahydrofuran (160 mL) was treated with isothiocyanatotrimethylsilane (66 mL, 470 mmol) and heated at reflux under nitrogen. After 15 h, the reaction mixture was cooled to ambient temperature and quenched by cautious addition of a saturated aqueous sodium bicarbonate solution (470 mL). The resulting mixture was extracted with dichloromethane, and the aqueous phase was extracted twice more with dichloromethane. The combined organic layers were dried (Na₂SO₄) and concentrated under reduced pressure to afford a yellow-amber foam, which was purified by chromatography on silica gel, eluting with 0–80% ethyl acetate in heptanes to afford 49.2 g of a solid. This solid was resuspended in equal parts of ethyl acetate and heptane before being heated at 70 °C for 1 h and then stirred at ambient temperature for 1 h. The resulting solid was collected by vacuum filtration, rinsing the material with additional 1:1 ethyl acetate/heptane, to afford **25** as a colorless fine powder (38.3 g, 59.5%). ¹H NMR (500 MHz, CDCl₃, major rotamer) δ 9.58 (br s, 1 H), 7.26 (d, $J = 8.4$ Hz, 1 H), 6.59 (dd, $J = 8.4, 2.1$ Hz, 1 H), 6.51 (d, J

= 2.2 Hz, 1 H), 5.81 (d, $J = 2.2$ Hz, 1 H), 4.68–4.81 (m, 2 H), 3.87 (s, 3 H), 3.84 (s, 3 H), 3.74 (dt, $J = 14.4, 5.4$ Hz, 1 H), 3.23–3.45 (m, 2 H), 1.40 (s, 9 H). LCMS (ESI⁺) m/z : 408.3 [M + H]⁺ (100%).

1-(2-Aminoethyl)-6-(2,4-dimethoxyphenyl)-2-thioxo-2,3-dihydropyrimidin-4(1H)-one Hydrochloride (4). Acetyl chloride (55 mL, 770 mmol) was added slowly over 3 min to a solution of ethanol (50 mL, 860 mmol) in ethyl acetate (390 mL), cooled by stirring in an ice/water bath. After 5 min, the cooling bath was removed, and the solution was stirred for an additional 45 min before being added to *tert*-butyl 2-(6-(2,4-dimethoxyphenyl)-4-oxo-2-thioxo-3,4-dihydropyrimidin-1(2H)-yl)ethylcarbamate (**25**) (31.7 g, 77.8 mmol). After stirring for 5 h, the resulting solid was collected by vacuum filtration, rinsing with ethyl acetate. The material collected was dried under vacuum to afford 26.6 g (99.3%) of the desired product **4** as a colorless solid. ¹H NMR (500 MHz, CD₃OD) δ 7.27 (d, $J = 8.3$ Hz, 1 H), 6.73 (d, $J = 2.2$ Hz, 1 H), 6.70 (dd, $J = 8.3, 2.2$ Hz, 1 H), 5.80 (s, 1 H), 4.82 (ddd, $J = 14.0, 7.7, 6.4$ Hz, 1 H), 4.14 (ddd, $J = 14.0, 7.8, 5.9$ Hz, 1 H), 3.89 (s, 3 H), 3.87 (s, 3 H), 3.12 (ddd, $J = 12.9, 7.7, 6.4$ Hz, 1 H), 3.06 (ddd, $J = 12.9, 7.8, 5.9$ Hz, 1 H). LCMS (ESI⁺) m/z : 291.3 [M – NH₃ + H]⁺ (100%), 308.3 [M + H]⁺ (33%), 615.5 [2M + H]⁺ (2.3%). HRMS: m/z calcd for C₁₄H₁₈N₃O₃S [M + H]⁺ 308.1069, found 308.1059. HPLC purity: >95%.

Methyl (Z)-3-(2,4-Dimethoxyphenyl)-3-((2-isopropoxyethyl)amino)acrylate (21). A solution of methyl 3-(2,4-dimethoxyphenyl)-3-oxopropanoate (**10**) (40.0 g, 168 mmol) and 2-aminoacetamide hydrochloride (**16**) (49.4 g, 447 mmol) in methanol (160 mL) was agitated with the aid of a mechanical stirrer as it was treated with triethylamine (48 mL, 344 mmol) followed by acetic acid (24 mL, 380 mmol) and then heated in a 80 °C oil bath. After 16 h, the mixture was allowed to cool to ambient temperature, treated with water (200 mL), and stirred for 1 h. The resulting solids were collected by filtration and resuspended in methyl *tert*-butyl ether (300 mL), filtered, and dried under a flow of nitrogen gas for 16 h to afford **21** as a flocculent colorless solid (41.2 g, 83%). ¹H NMR (400 MHz, CDCl₃) δ 8.77 (t, $J = 5.4$ Hz, 1 H), 7.13 (d, $J = 8.3$ Hz, 1 H), 6.47–6.52 (m, 2H), 4.53 (s, 1 H), 3.84 (s, 3 H), 3.82 (s, 3 H), 3.66 (s, 3H), 3.61 (td, $J = 5.5, 5.5$ Hz, 2 H), 3.15 (td, $J = 5.5, 5.5$ Hz, 2 H).

2-(6-(2,4-Dimethoxyphenyl)-4-oxo-2-thioxo-3,4-dihydropyrimidin-1(2H)-yl)acetamide (5). A suspension of methyl (Z)-3-(2,4-dimethoxyphenyl)-3-((2-isopropoxyethyl)amino)acrylate (**21**, 41.2 g, 140 mmol) in 2-methyltetrahydrofuran (200 mL) was treated with isothiocyanatotrimethylsilane (95 mL, 630 mmol) and then heated at 80 °C for 16 h before the temperature was increased to 100 °C. After an additional 24 h, the reaction mixture was cooled to ambient temperature, diluted with methyl *tert*-butyl ether (300 mL), and the resulting solid material was collected by vacuum filtration, rinsing with methyl *tert*-butyl ether, before drying under a stream of nitrogen gas. The solid was then dissolved in an aqueous 1 N NaOH solution (600 mL) and extracted twice with dichloromethane. The organic phases were discarded, and the aqueous layer was cooled in an ice bath before being acidified with concentrated aqueous HCl. A precipitate began to form at pH ≈ 7 as the solution was acidified further until pH = 2. The resulting solid material was collected by vacuum filtration, rinsing with water, and dried under a stream of nitrogen gas to afford the title compound **5** as a tan solid (27.8 g, 62%). ¹H NMR (500 MHz, DMSO-*d*₆) δ 12.75 (s, 1 H), 7.31 (br s, 1 H), 7.08 (d, $J = 8.54$ Hz, 1 H), 6.98 (br s, 1 H), 6.69 (d, $J = 2.20$ Hz, 1 H), 6.61 (dd, $J = 8.54, 2.20$ Hz, 1 H), 5.74 (s, 1 H), 5.38 (br s, 1 H), 3.87 (br s, 1 H), 3.82 (s, 3 H), 3.81 (s, 3 H). MS (ES⁺) m/z : 322.2 [M + H]⁺. HRMS: m/z calcd for C₁₄H₁₆N₃O₄S [M + H]⁺ 322.0862, found 322.0856. Anal. Calcd for C₁₄H₁₅N₃O₄S: C, 52.33; H, 4.71; N, 13.08; S, 9.98. Found: C, 52.09; H, 4.56; N, 12.86; S, 9.94. HPLC purity: 94.8%.

Methyl (Z)-3-(2,4-Dimethoxyphenyl)-3-((2-ethoxy-2-oxoethyl)amino)acrylate (22). A solution of methyl 3-(2,4-dimethoxyphenyl)-3-oxopropanoate (**10**) (5.0 g, 21 mmol), glycine methyl ester hydrochloride (**17**) (10.5 g, 83.9 mmol), acetic acid (1.20 mL, 21 mmol), and triethylamine (8.5 g, 83.9 mmol) in ethanol (30 mL) was heated at 100 °C for 18 h. The reaction mixture was allowed to cool to ambient temperature and partitioned between EtOAc and saturated aqueous ammonium chloride. The organic layer was

separated, washed with brine, dried over sodium sulfate, and concentrated under reduced pressure. The residue was dissolved in dichloromethane (10 mL) and eluted through a column of silica gel with a gradient of ethyl acetate in heptanes (15–35%) to afford **22** as a yellow solid (4.7 g, 69%). The material was used directly in the next step without further purification. $^1\text{H NMR}$ (400 MHz, CDCl_3) δ 8.95 (br s, 1 H), 7.14 (d, $J = 10.57$ Hz, 1 H), 6.49 (dd, $J = 8.28, 2.07$ Hz, 1 H), 6.46 (d, $J = 2.07$, 1 H), 4.60 (s, 1 H), 4.16 (q, $J = 7.80$ Hz, 2 H), 3.83 (s, 3 H), 3.80 (s, 3 H), 3.69 (s, 3 H), 1.24 (t, $J = 7.80$ Hz, 3 H). MS (ES^+) m/z : 324.3 [$\text{M} + 1$] $^+$.

Ethyl 2-(6-(2,4-Dimethoxyphenyl)-4-oxo-2-thioxo-3,4-dihydropyrimidin-1(2H)-yl)acetate (26). A solution of methyl (Z)-3-(2,4-dimethoxyphenyl)-3-((2-ethoxy-2-oxoethyl)amino)acrylate (**22**) (4.68 g, 15.1 mmol) in 2-methyltetrahydrofuran (38 mL) was treated with isothiocyanatotrimethylsilane (12.9 mL, 90.8 mmol), and the solution was purged with nitrogen gas and heated at 110 °C. After 18 h, the mixture was allowed to cool to ambient temperature and concentrated under reduced pressure to afford a red solid, which was then suspended in 200 mL of a 25% ethyl acetate in heptanes mixture. After stirring at room temperature for 1 h, the solid was collected by filtration and then triturated with methylene chloride (100 mL), concentrated under reduced pressure, and dried under vacuum to afford **26** (4.42 g, 87%) as a pink solid. This material was used directly in the next step without further purification. $^1\text{H NMR}$ (500 MHz, CDCl_3) δ 9.91 (br s, 1 H), 7.13 (d, $J = 6.12$ Hz, 1 H), 6.54 (s, 1 H), 6.51 (d, $J = 6.12$ Hz, 1 H), 5.86 (s, 1 H), 5.44–5.40 (m, 1 H), 4.25–4.20 (m, 1 H), 4.16–4.06 (m, 2 H), 3.86 (s, 3 H), 3.83 (s, 3 H), 1.20 (t, $J = 6.12$ Hz, 3 H). MS (ES^+) m/z : 351.5 [$\text{M} + \text{H}$] $^+$.

2-(6-(2,4-Dimethoxyphenyl)-4-oxo-2-thioxo-3,4-dihydropyrimidin-1(2H)-yl)acetic Acid (27). A solution of ethyl 2-(6-(2,4-dimethoxyphenyl)-4-oxo-2-thioxo-3,4-dihydropyrimidin-1(2H)-yl)acetate (**26**) (6.8 g, 20.3 mmol) in methanol (34 mL) was treated with a 6 N aqueous NaOH solution (16.9 mL), and the solution was heated at 35 °C. After 3 h, the reaction mixture was allowed to cool to ambient temperature and concentrated under reduced pressure. The residue was combined with water (100 mL) and extracted with ethyl acetate (2 \times 200 mL), and the aqueous phase was acidified to pH \approx 2 with concentrated aqueous HCl. The acidic aqueous solution was extracted with ethyl acetate (3 \times 200 mL), and the combined organic phases were dried (Na_2SO_4) and concentrated under reduced pressure to afford 6.53 g (99%) of **27** as a colorless solid. $^1\text{H NMR}$ (500 MHz, CD_3OD) δ 7.16 (d, $J = 8.86$ Hz, 1 H), 6.67 (s, 1 H), 6.64 (d, $J = 8.86$ Hz, 1 H), 5.79 (s, 1 H), 5.52–5.40 (m, 1 H), 4.34–4.19 (m, 1 H), 3.87 (s, 3 H), 3.86 (s, 3 H). MS (ES^+) m/z : 323.2 [$\text{M} + \text{H}$] $^+$.

tert-Butyl 2-(2-(6-(2,4-Dimethoxyphenyl)-4-oxo-2-thioxo-3,4-dihydropyrimidin-1(2H)-yl)acetamido)ethyl)carbamate (28). A solution of 2-(6-(2,4-dimethoxyphenyl)-4-oxo-2-thioxo-3,4-dihydropyrimidin-1(2H)-yl)acetic acid (**27**) (40 g, 124 mmol) in DMF (300 mL) was treated with *tert*-butyl-(2-aminoethyl)carbamate (40 g, 250 mmol) and pyridine (30 mL) and cooled to 0 °C under nitrogen. A 50% solution of 2,4,6-tripropyl-1,3,5,2,4,6-trioxatriphosphorinane 2,4,6-trioxide in DMF (109 mL) was carefully added with stirring. After 1 h, the cooling bath was removed and the reaction mixture was stirred at ambient temperature. After 4 h, the solution was poured slowly into a stirring 0.5 M aqueous HCl solution (2500 mL). After stirring at ambient temperature for 1 h, the resulting solid was collected by vacuum filtration. The solid was washed with 0.5 M aqueous HCl (500 mL) followed by water (500 mL). The resulting solid was dried in a vacuum oven at 50 °C for 20 h to afford 54.6 g of light beige powder. This solid was suspended in ethyl acetate (500 mL), heated to 70 °C under a stream of nitrogen gas with stirring for 1 h, and then allowed to cool to ambient temperature with stirring. After 18 h, the suspension was cooled to 0 °C, the solid was collected by vacuum filtration, the filter cake washed with cold (0 °C) ethyl acetate (100 mL) and dried in the vacuum oven at 50 °C for 9 h to afford 49.0 g of an off-white solid. This solid was suspended in acetonitrile (300 mL) and stirred at 70 °C under a stream of nitrogen for 18 h. The mixture was cooled to 0 °C, and the resultant solid was collected by vacuum filtration, washed with cold acetonitrile (50 mL), and dried in a vacuum oven at 50 °C for 8 h to give 46.5 g of off-white solid. This

solid was suspended in ethyl acetate (350 mL), heated to 70 °C under a stream of nitrogen gas with stirring for 1 h and then at ambient temperature for 18 h before the suspension was cooled down to 0 °C, and the solid was collected by vacuum filtration, the filter cake washed with cold (0 °C) ethyl acetate (50 mL) and dried in the vacuum oven at 50 °C for 9 h to give **28** (45.4 g, 78.8%) as an off-white powder. $^1\text{H NMR}$ (500 MHz, CD_3OD) δ 8.99 (br s, 1 H), 7.16 (d, $J = 7.65$ Hz, 1 H), 6.65 (s, 1 H), 6.62 (d, $J = 7.65$ Hz, 1 H), 5.78 (s, 1 H), 5.51–5.41 (m, 1 H), 4.22–4.14 (m, 1 H), 3.87 (s, 3 H), 3.85 (s, 3 H), 3.19–3.11 (m, 2 H), 3.06–3.00 (m, 2 H), 1.42 (s, 9 H). MS (ES^+) m/z : 465.3 [$\text{M} + \text{H}$] $^+$.

N-(2-Aminoethyl)-2-(6-(2,4-dimethoxyphenyl)-4-oxo-2-thioxo-3,4-dihydropyrimidin-1(2H)-yl)acetamide Hydrochloride (6). Ethanol (21.5 mL), cooled at 0 °C under nitrogen, was slowly treated with acetyl chloride (1.55 mL) over 5 min, after which the reaction mixture was heated at 50 °C. After 30 min, the reaction mixture was cooled to ambient temperature and *tert*-butyl-(2-(6-(2,4-dimethoxyphenyl)-4-oxo-2-thioxo-3,4-dihydropyrimidin-1(2H)-yl)acetamido)ethyl)carbamate (**28**) (1.0 g, 2.15 mmol) was added, followed by heating to 50 °C. After 1 h, the reaction mixture was cooled to ambient temperature and concentrated under reduced pressure. The resulting residue was then suspended in ethanol (10 mL), heated at 75 °C for 20 min before adding ethyl acetate (20 mL). After heating for another 20 min, the reaction mixture was allowed to gradually cool to ambient temperature with stirring. After 18 h, the resulting precipitate was filtered and dried in a vacuum oven at 70 °C for 20 h to afford **6** (751 mg, 87%) as a colorless solid. $^1\text{H NMR}$ (500 MHz, $\text{DMSO}-d_6$) δ 12.81 (br s, 1 H), 8.26 (br s, 1 H), 8.01 (br s, 2 H), 7.08 (d, $J = 7.91$ Hz, 1 H), 6.70 (s, 1 H), 6.62 (d, $J = 7.91$ Hz, 1 H), 5.78 (s, 1 H), 5.41–5.35 (m, 1 H), 4.07–4.02 (m, 1 H), 3.84 (s, 3 H), 3.83 (s, 3 H), 3.20–3.16 (m, 2 H), 2.74–2.64 (m, 2 H). MS (ES^+) m/z : 365.2 [$\text{M} + \text{H}$] $^+$. HRMS: m/z calcd for $\text{C}_{16}\text{H}_{21}\text{N}_4\text{O}_4\text{S}$ [$\text{M} + \text{H}$] $^+$ 365.1284, found 365.1278. HPLC purity: >95%.

Sodium 1-(2,5-Dimethoxyphenyl)-3-ethoxy-3-oxoprop-1-en-1-olate (11). A 20 L reaction vessel was charged with magnesium ethoxide (413.5 g, 3.61 mol) and THF (6.6 L), and the resulting mixture was treated with ethyl hydrogen malonate (**29**) (888.9 mL, 7.23 mol) in THF (20 mL) and heated at 45 °C for 4 h. Meanwhile, a 20 L reactor was charged with 2,5-dimethoxybenzoic acid (**30**) (600 g, 3.29 mol) and THF (3.6 L). To this mixture was added 1,1'-carbonyldiimidazole (585.98 g, 3.61 mol) in portions to avoid excess foaming. After stirring for 3 h at ambient temperature, the solution of activated acid was added gradually to the ethyl malonate solution and the combined reaction mixture was heated at 45 °C. After 20 h, the mixture was concentrated under reduced pressure followed by the addition of ethyl acetate (6 L) and 2 N HCl (3 L). After mixing, the layers were separated and the organic phase was washed sequentially with 2 N HCl (3 L), saturated sodium bicarbonate (3 L), and water (3 L). The organic phase was concentrated under reduced pressure, the residue taken up in ethyl acetate (6 L) and concentrated again to afford an oil, which was transferred to a 20 L reaction vessel with 5 L of ethyl acetate and treated with a 4.35 M solution of sodium methoxide (793 mL, 3.45 mol) in methanol. After stirring at room temperature for 3 h, an additional 6 L of ethyl acetate was added, the solid was collected by vacuum filtration and dried overnight in a vacuum oven at 40 °C to give 661 g of **11** (73%) as a solid. $^1\text{H NMR}$ (400 MHz, $\text{DMSO}-d_6$) δ 6.92 (d, $J = 3.0$ Hz, 1 H), 6.84 (d, $J = 8.8$ Hz, 1 H), 6.73 (dd, $J = 8.8, 3.0$ Hz, 1 H), 4.67 (s, 1 H), 3.88 (q, $J = 7.0$ Hz, 2 H), 3.67 (s, 6 H), 1.12 (t, $J = 7.0$ Hz, 3 H). MS (ES^+) m/z : 253.1 [$\text{M} + \text{H}$] $^+$.

Ethyl (Z)-3-((2-Amino-2-oxoethyl)amino)-3-(2,5-dimethoxyphenyl)acrylate (23). A 5 L reaction vessel was charged with methanol (3.3 L), sodium methoxide (102.4 g, 1.8 mol), and aminoacetamide hydrochloride (**16**) (202 g, 1.8 mol). The mixture was heated at 65 °C for 1 h before cooling to 50 °C and adding acetic acid (30.88 g, 29.47 mL, 514.25 mmol) and sodium 1-(2,5-dimethoxyphenyl)-3-ethoxy-3-oxoprop-1-en-1-olate (**11**) (300 g, 1.09 mol). After heating at reflux for 16 h, the reaction mixture was cooled to 10 °C, stirred for 30 min, the resulting solid collected by filtration and dried in a vacuum oven for 14 h to afford **23** (339.4 g, 100%) as a

solid. $^1\text{H NMR}$ (400 MHz, DMSO- d_6) δ 8.84 (t, $J = 4.7$ Hz, 1 H), 7.36 (s, 1 H), 7.09 (s, 1 H), 7.02 (d, $J = 8.9$ Hz, 1 H), 6.97 (dd, $J = 8.9, 2.8$ Hz, 1 H), 6.74 (d, $J = 2.8$ Hz, 1 H), 4.31 (s, 1 H), 4.03 (q, $J = 7.1$ Hz, 2 H), 3.74 (s, 6 H), 3.58 (br s, 1 H), 3.47 (br s, 1 H), 1.18 (t, $J = 7.1$ Hz, 3 H). MS (ES $^+$) m/z : 309.1 [M + H] $^+$.

2-(6-(2,5-Dimethoxyphenyl)-4-oxo-2-thioxo-3,4-dihydropyrimidin-1(2H)-yl)acetamide (7). A 5 L reaction vessel equipped with an efficient stirrer was charged with ethyl (Z)-3-((2-amino-2-oxoethyl)amino)-3-(2,5-dimethoxyphenyl)acrylate (**23**) (400 g, 1.30 mol), butyl acetate (3.4 L), and isothiocyanatotrimethylsilane (585.67 mL, 544.96 g, 4.15 mol), and the mixture was heated to reflux. After 16 h, the mixture was cooled to 40 °C and treated with a solution of 2 N aqueous NaOH (1.95 L). The organic layer was separated and extracted with another portion of 2 N aqueous NaOH (0.32 L). The combined aqueous phases were filtered, extracted twice with dichloromethane (2 \times 1.6 L), and added slowly to a well-stirred 3 N aqueous HCl solution (1.3 L) at room temperature. After stirring for 30 min, the resulting solid was filtered and dissolved in dimethylformamide (2.4 L) at 90 °C and before water (2 L) was added slowly to the solution. The mixture was cooled gradually to room temperature and the resulting solid isolated by vacuum filtration, rinsing with water. This solid was then suspended in 1.25 L of methanol and stirred as 1.25 L of water was added. The mixture was heated with stirring at 50 °C for 2 h and then cooled to 10 °C for 2 h before collecting the solid by vacuum filtration and drying in a vacuum oven to afford **7** (245 g, 59%) as a solid. $^1\text{H NMR}$ (500 MHz, DMSO- d_6) δ 12.80 (s, 1 H), 7.32 (br s, 1 H), 7.06–7.11 (m, 2 H), 7.06 (br s, 1 H), 6.74–6.77 (m, 1 H), 5.82 (d, $J = 2.20$ Hz, 1 H), 5.37 (br s, 1 H), 3.88 (br s, 1 H), 3.78 (s, 3 H), 3.70 (s, 3 H). MS (ES $^+$) m/z : 322.2 [M + H] $^+$. HRMS: m/z calcd for $\text{C}_{14}\text{H}_{16}\text{N}_3\text{O}_4\text{S}$ [M + H] $^+$ 322.0862, found 322.0856. HPLC purity: >95%.

Ethyl 3-(5-Chloro-2-methoxyphenyl)-3-oxopropanoate (12). A 3 L three-necked round-bottomed flask, flushed with nitrogen, was charged with magnesium ethoxide (67.46 g, 589.51 mmol) and THF (1100 mL), and the resulting mixture was stirred as ethyl hydrogen malonate (**29**) (162.26 g, 1.18 mol) in THF (100 mL) was added and the mixture was heated at 45 °C for 4 h. Meanwhile, a 2 L three-necked round-bottomed flask, flushed with nitrogen, was charged with 5-chloro-2-methoxybenzoic acid (**31**) (100 g, 536 mmol) and THF (600 mL). To this mixture was added 1,1'-carbonyldiimidazole (95.59 g, 589.5 mmol) in portions to avoid excess foaming. After stirring for 3 h, the solution of activated acid was added gradually to the ethyl malonate solution, and the resulting reaction mixture was heated at 45 °C. After 20 h, the reaction mixture was concentrated under reduced pressure before adding ethyl acetate (1 L) followed by 2 N HCl (500 mL). After mixing, the layers were separated and the organic phase was washed sequentially with 2 N HCl (500 mL), saturated sodium bicarbonate (500 mL), and water (500 mL). The organic phase was concentrated under reduced pressure to afford **12** (104.94 g, 76%) as a solid. $^1\text{H NMR}$ showed the desired product as a 7.5:1 keto/enol mixture. For the keto tautomer: $^1\text{H NMR}$ (500 MHz, CDCl_3) δ 7.85 (d, $J = 2.93$ Hz, 1 H), 7.45 (dd, $J = 8.90, 2.81$ Hz, 1 H), 6.92 (d, $J = 8.78$ Hz, 1 H), 4.18 (q, $J = 7.16$ Hz, 2 H), 3.95 (s, 2 H), 3.90 (s, 3 H), 1.24 (t, $J = 7.07$ Hz, 3 H). MS (ES $^+$) m/z : 257.2 [M + H] $^+$.

Ethyl (Z)-3-((2-Amino-2-oxoethyl)amino)-3-(5-chloro-2-methoxyphenyl)acrylate (24). A 5 L reaction vessel was charged with methanol (3.3 L), sodium methoxide (102.4 g, 1.8 mol), and aminoacetamide hydrochloride (**16**) (202 g, 1.8 mol). The mixture was heated at 65 °C for 1 h before cooling to 50 °C and adding acetic acid (514.3 mmol, 30.9 g, 29.5 mL) and ethyl 3-(5-chloro-2-methoxyphenyl)-3-oxopropanoate (**12**) (300 g, 1.17 mol). After heating at reflux for 16 h, the reaction mixture was stirred as it was cooled to 10 °C. After 30 min the resulting solid was filtered and dried in a vacuum oven (20 mmHg, 65 °C) for 14 h to afford **24** (339.4 g, 93%) as a solid. $^1\text{H NMR}$ (500 MHz, DMSO- d_6) δ 8.80 (t, $J = 5.00$ Hz, 1 H), 7.47 (dd, $J = 8.90, 2.81$ Hz, 1 H), 7.27 (br s, 1 H), 7.22 (d, $J = 2.68$ Hz, 1 H), 7.14 (d, $J = 8.78$ Hz, 1 H), 7.09 (br s, 1 H), 4.30 (s, 1 H), 4.03 (q, $J = 7.07$ Hz, 2 H), 3.80 (s, 3 H), 3.56 (br s, 1 H), 3.45 (br s, 1 H), 1.18 (t, $J = 7.07$ Hz, 3 H). MS (ES $^+$) m/z : 313.2 [M + H] $^+$.

2-(6-(5-Chloro-2-methoxyphenyl)-4-oxo-2-thioxo-3,4-dihydropyrimidin-1(2H)-yl)acetamide (8). A reaction vessel equipped with an efficient stirrer was charged with ethyl (Z)-3-((2-amino-2-oxoethyl)amino)-3-(5-chloro-2-methoxyphenyl)acrylate (**24**) (15 g, 50.2 mmol), butyl acetate (150 mL), and isothiocyanatotrimethylsilane (21.1 g, 22.7 mL, 160.7 mmol), and the mixture was heated to reflux. After 15 h, the mixture was cooled to 30 °C and treated with 1 N aqueous NaOH (112.5 mL). After 30 min, the organic layer was separated and extracted with another portion of 1 N sodium hydroxide (37.5 mL). The combined aqueous phases were extracted twice with dichloromethane (2 \times 45 mL), filtered, and treated with 6 N HCl until a pH of 2.5 was achieved. After stirring for 1 h, the resulting solid was collected by vacuum filtration, resuspended in 100 mL of a 1:1 methanol–water solution, heated with stirring at 50 °C for 2 h, and cooled to room temperature before collecting the solid by filtration and drying in a vacuum oven (20 mmHg, 50 °C) for 12 h to afford **8** (8.7 g, 53%) as a tan solid (mp = 165.3 °C). $^1\text{H NMR}$ (500 MHz, DMSO- d_6) δ 12.85 (s, 1 H), 7.57 (dd, $J = 9.03, 2.68$ Hz, 1 H), 7.33 (s, 1 H), 7.17–7.23 (m, 2 H), 7.10 (s, 1 H), 5.89 (d, $J = 1.71$ Hz, 1 H), 5.41 (br s, 1 H), 3.89 (br s, 1 H), 3.84 (s, 3 H). MS (ES $^+$) m/z : 326.0 [M + H] $^+$. HRMS: m/z calcd for $\text{C}_{13}\text{H}_{13}\text{ClN}_3\text{O}_3\text{S}$ [M + H] $^+$ 326.0366, found 326.0361. Anal. Calcd for $\text{C}_{13}\text{H}_{12}\text{ClN}_3\text{O}_3\text{S}$: C, 47.93; H, 3.71; N, 12.90; S, 9.84. Found: C, 47.81; H, 3.70; N, 12.83; S, 9.83. HPLC purity: >95%.

Pharmacokinetics. All experiments involving animals were conducted in our AAALAC-accredited facilities and were reviewed and approved by Pfizer Institutional Animal Care and Use Committee. Male CD-1 mice (25–35 g), jugular vein/carotid artery double cannulated Wistar-Han rats (250 g), obtained from Charles River Laboratories (Wilmington, MA), male beagle dogs (12 kg), and male cynomolgus monkeys (7 kg) were used for these studies. Animals were fasted overnight and fed after dosing (1.0 or 2.0 h), whereas access to water was provided ad libitum. Compounds were administered intravenously (iv) in either saline, 12% sulfobutyl ether β -cyclodextrin with or without 1% DMSO or 30% hydroxypropyl- β -cyclodextrin containing 5% DMSO via the tail vein (mice, $n = 3$), carotid artery (rats, $n = 3$), saphenous vein (dogs, $n = 3$), femoral vein (monkeys, $n = 2$) at a dose of 1.0 mg/kg in a dosing volume of 5 mL/kg (mice), 2 mL/kg (rats), 0.5 mL/kg (dogs), and 1 mL/kg (monkeys). Serial blood samples were collected before dosing and 0.083, 0.25, 0.5, 1, 2, 4, 7, and 24 h after dosing. Compounds were also administered by po gavage to mice (5 mg/kg at 5 mL/kg in 0.5% methylcellulose), rats (5 mg/kg at 5 mL/kg in 0.5% methylcellulose), dogs (3 mg/kg at 1.5 mL/kg in 0.5% methylcellulose), and monkeys (3 mg/kg at 5 mL/kg in 0.5% methylcellulose). Blood samples were taken prior to po administration, and then serial samples were collected at 0.25, 0.5, 1, 2, 4, 7, and 24 h after dosing. Blood samples from the various pharmacokinetic studies were centrifuged to generate plasma. All plasma samples were kept frozen until analysis. Urine samples (0–7.0 and 7.0–24 h; pooled 0–24 h for mice) were also collected after iv administration to mice, rats, dogs, and monkeys. For mouse samples, aliquots of plasma (10 μL) or urine (2 μL mixed with 8 μL plasma) were extracted using liquid/liquid extraction with methyl *tert*-butyl ether containing internal standard. For rat, dog, or monkey samples, aliquots of plasma or urine (20–25 μL) were transferred to 96-well blocks and acetonitrile (150–200 μL) containing internal standard was added to each well. Supernatant was dried under nitrogen and reconstituted with 100 μL of acetonitrile/water (1:1 with 0.1% formic acid for mice; 20:80 for dog) or added to 100 μL of water without evaporation (rat, monkey). Following extraction, the samples were then analyzed by LC–MS/MS, and concentrations of analyte in plasma and urine were determined by interpolation from a standard curve as described previously.³⁹

In Vitro Metabolism of N1-Substituted-6-arylthiouracils in MPO. Stock solutions of thiouracil derivatives were prepared in DMSO. Compounds (final concentration of 10 μM) were added to an incubation mixture containing 50 mM sodium phosphate buffer, pH 7.4, 150 mM NaCl, 1 mM diethylenetriaminepentaacetic acid, 2 μM H_2O_2 , 30 μM Amplex Red, and 1 mM GSH. Reactions were initiated by the addition of 100 pM MPO, and the final concentration of

DMSO was kept at 2% in the incubation (volume of 200 μL). The reaction mixture was incubated at 37 °C for 60 min, terminated by the addition of ice cold acetonitrile (400 μL) and centrifuged (3000g, 15 min). The supernatants were dried under a steady stream of nitrogen, reconstituted with 25% aqueous acetonitrile (250 μL), and analyzed via LC–MS/MS for formation of sulfhydryl conjugates. Qualitative assessment of metabolites was conducted using a Thermo Finnegan Surveyor photodiode array plus detector, Thermo Acela pump, and a Thermo Acela autosampler (ThermoScientific, West Palm Beach, FL). Chromatography was performed on a Phenomenex Hydro RP C18 (4.6 mm \times 150 mm, 3.5 μm) column (Phenomenex, Torrance, CA). The mobile phase was composed of 5 mM ammonium formate buffer with 0.1% formic acid (pH = 3) (solvent A) and acetonitrile (solvent B) at a flow rate of 1 mL/min. The binary gradient was as follows: solvent A to solvent B ratio was held at 95:5 (v/v) for 3 min and then adjusted to 55:45 (v/v) from 0 to 35 min, 30:70 (v/v) from 35 to 45 min, and 5:95 (v/v) from 45 to 52 min where it was held for 3 min and then returned to 95:5 (v/v) for 6 min before next analytical run. Metabolite identification was performed on a Thermo Orbitrap mass spectrometer operating in positive ion electrospray mode. The spray potential was 4 V, and heated capillary was at 275 °C. Xcalibur software version 2.0 was used to control the HPLC–MS system. Full scan measurements from 50–1000 amu were collected at 15 000 resolution, with two data-dependent acquisition scans of the most intense ion in scan events 1 and 2, respectively. Product ion spectra were acquired at a normalized collision energy of 65 eV with an isolation width of 2 amu.

Liquid chromatography–tandem mass spectrometry (LC–MS/MS) analysis of an incubation of arylthiourea **2** (retention time (t_{R}) = 25.4 min, exact mass (MH^+) = 351.1367) with human MPO/ $\text{H}_2\text{O}_2/\text{Cl}^-$ in the presence of excess glutathione (GSH) (1 mM) indicated the formation of a GSH conjugate (t_{R} = 15.7 min; MH^+ = 624.2334, m/z ($+\text{H}^+$) = 495.1906 (loss of pyroglutamate, 129 amu), which can be obtained via oxidation of the thiocarbonyl group in **2** to the putative sulfonate species followed by nucleophilic displacement in the presence of exogenously added GSH (Scheme 2).

Inhibition of MPO Activity in LPS-Treated Cynomolgus Monkeys by 8. All experiments involving animals were conducted in our AAALAC-accredited facilities and were reviewed and approved by Pfizer Institutional Animal Care and Use Committee. Male cynomolgus monkeys ($n = 8$; >2.5 years old at initiation of dosing) were assigned to dose groups randomized in a crossover manner with 2 weeks between treatments. The treatments were the following: iv LPS (5 $\mu\text{g}/\text{kg}$; Sigma, L3491) in sterile saline followed after 1 h by po administration of vehicle (20 mM Tris, 0.5% [w/v] hydroxypropylmethylcellulose, and 0.5% [w/v] hydroxypropylmethylcellulose acetate succinate high-fine grade) or **8** in vehicle at 5, 20, or 80 mg/kg. Blood samples were taken just prior to LPS dosing and at 0.5, 2.0, 4.0, 8.0, and 24 h after vehicle or **8** dosing in sodium heparinized containers. Total MPO and residual MPO activity were determined from plasma samples by antibody capture as described above for the human whole blood assay, and plasma levels of **8** were measured by liquid chromatography–tandem mass spectrometry.

AUTHOR INFORMATION

Corresponding Author

*Phone: 860-441-3535. E-mail: Roger.B.Ruggeri@pfizer.com.

Author Contributions

The manuscript was written through contributions of all authors. All authors have given approval to the final version of the manuscript.

Notes

The authors declare the following competing financial interest(s): All authors are current or former employees of Pfizer, Inc.

ABBREVIATIONS USED

MPO, myeloperoxidase; H_2O_2 , hydrogen peroxide; COPD, chronic obstructive pulmonary disease; TPO, thyroid peroxidase; CYP, cytochrome P450; PF-06282999, 2-(6-(5-chloro-2-methoxyphenyl)-4-oxo-2-thioxo-3,4-dihydropyrimidin-1(2H)-yl)acetamide; po, oral; THF, tetrahydrofuran; LPS, lipopolysaccharide; PTU, propylthiouracil; k_{inact} , maximal rate of MPO inactivation; K_{i} , concentration required to achieve half the maximal rate of inactivator; $[\text{I}]$, inhibitor concentration; TMSNCS, isothiocyanatotrimethylsilane; T3P, 2,4,6-tripropyl-1,3,5,2,4,6-trioxatriphosphorinane 2,4,6-trioxide; LC–MS/MS, liquid chromatography–tandem mass spectrometry; GSH, glutathione; ADME, absorption, distribution, metabolism, and excretion; HLM, human liver microsome; HHEP, cryopreserved human hepatocyte; RRCK, Ralph–Russ canine kidney; iv, intravenous; CL_{p} , plasma clearance; V_{dss} , steady state volume of distribution; $t_{1/2}$, elimination half-life; T_{max} , time to reach C_{max}

REFERENCES

- (1) Hansson, M.; Olsson, I.; Nauseef, W. M. Biosynthesis, processing, and sorting of human myeloperoxidase. *Arch. Biochem. Biophys.* **2006**, *445*, 214–224.
- (2) Kutter, D. Prevalence of myeloperoxidase deficiency: Population studies using Bayer-Technicon automated hematology. *J. Mol. Med.* **1998**, *76*, 669–675.
- (3) Lekstrom-Himes, J.; Gallin, J. Immunodeficiency diseases caused by defects in phagocytes. *N. Engl. J. Med.* **2000**, *343*, 1703–1714.
- (4) Churg, A.; Marshall, C. V.; Sin, D. D.; Bolton, S.; Zhou, S.; Thain, K.; Cadogan, E. B.; Maltby, J.; Soars, M. G.; Mallinder, P. R.; Wright, J. L. Late intervention with a myeloperoxidase inhibitor stops progression of experimental chronic obstructive pulmonary disease. *Am. J. Respir. Crit. Care Med.* **2012**, *185*, 34–43.
- (5) Odobasic, D.; Yang, Y.; Muljadi, R. C.; O'Sullivan, K. M.; Kao, W.; Smith, M.; Morand, E. F.; Holdsworth, S. R. Endogenous myeloperoxidase is a mediator of joint inflammation and damage in experimental arthritis. *Arthritis Rheumatol.* **2014**, *66*, 907–917.
- (6) Odobasic, D.; Kitching, A. R.; Semple, T. J.; Holdsworth, S. R. Endogenous myeloperoxidase promotes neutrophil-mediated renal injury, but attenuates T cell immunity inducing crescentic glomerulonephritis. *J. Am. Soc. Nephrol.* **2007**, *18*, 760–770.
- (7) Choi, D. K.; Pennathur, S.; Perier, C.; Tieu, K.; Teismann, P.; Wu, D. C.; Jackson-Lewis, V.; Vila, M.; Vonsattel, J. P.; Heinecke, J. W.; Przedborski, S. Ablation of the inflammatory enzyme myeloperoxidase mitigates features of Parkinson's disease in mice. *J. Neurosci.* **2005**, *25*, 6594–6600.
- (8) Mayyas, F. A.; Al-Jarrah, M. I.; Ibrahim, K. S.; Alzoubi, K. H. Level and significance of plasma myeloperoxidase and the neutrophil to lymphocyte ratio in patients with coronary artery disease. *Exp. Ther. Med.* **2014**, *8*, 1951–1957.
- (9) Zhang, R.; Brennan, M. L.; Fu, X. Association between myeloperoxidase levels and risk of coronary artery disease. *JAMA, J. Am. Med. Assoc.* **2001**, *286*, 2136–2142.
- (10) Ndrepepa, G.; Braun, S.; Mehili, J.; von Beckerath, N.; Schomig, A.; Kastrati, A. Myeloperoxidase level in patients with stable coronary artery disease and acute coronary syndromes. *Eur. J. Clin. Invest.* **2008**, *38*, 90–96.
- (11) Heinecke, J. W. Mechanisms of oxidative damage of low density lipoprotein in human atherosclerosis. *Curr. Opin. Lipidol.* **1997**, *8*, 268–274.
- (12) Smith, J. D. Myeloperoxidase, inflammation, and dysfunctional HDL. *J. Clin. Lipidol.* **2010**, *4*, 382–388.
- (13) Eiserich, J. P.; Baldus, S.; Brennan, M. L.; Ma, W.; Zhang, C.; Tousson, A.; Castro, L.; Lusa, A. J.; Nauseef, W. M.; White, C. R.; Freeman, B. A. Myeloperoxidase, a leukocyte-derived vascular NO oxidase. *Science* **2002**, *296*, 2391–2394.

- (14) Carr, A. C.; McCall, M. R.; Frei, B. Oxidation of LDL by myeloperoxidase and reactive nitrogen species: reaction pathways and antioxidant protection. *Arterioscler., Thromb., Vasc. Biol.* **2000**, *20*, 1716–1723.
- (15) Sepe, S. M.; Clark, R. A. Oxidant membrane injury by the neutrophil myeloperoxidase system. II. Injury by stimulated neutrophils and protection by lipid-soluble antioxidants. *J. Immunol.* **1985**, *134*, 1896–1901.
- (16) Askari, A. T.; Brennan, M. L.; Zhou, X.; Drinko, J.; Morehead, A.; Thomas, J. D.; Topol, E. J.; Hazen, S. L.; Penn, M. S. Myeloperoxidase and plasminogen activator inhibitor 1 play a central role in ventricular remodeling after myocardial infarction. *J. Exp. Med.* **2003**, *197*, 615–624.
- (17) Penn, M. S. The role of leukocyte-generated oxidants in left ventricular remodeling. *Am. J. Cardiol.* **2008**, *101*, S30–S33.
- (18) Openinnovation. AZD-5904. <http://openinnovation.astrazeneca.com/what-we-offer/compound/azd5904/> (accessed Aug 19, 2015).
- (19) AZD3241 PET MSA Trial, Phase 2, Randomized, 12 Week Safety and Tolerability Trial with PET in MSA Patients. <https://clinicaltrials.gov/ct2/show/NCT02388295> (accessed Aug 19, 2015).
- (20) Davies, M. J. Myeloperoxidase-derived oxidation: mechanisms of biological damage and its prevention. *J. Clin. Biochem. Nutr.* **2011**, *48*, 8–19.
- (21) Lobach, A. R.; Uetrecht, J. Involvement of myeloperoxidase and NADPH oxidase in the covalent binding of amodiaquine and clozapine to neutrophils: implications for drug-induced agranulocytosis. *Chem. Res. Toxicol.* **2014**, *27*, 699–709.
- (22) Svensson, B. E. Thiols as myeloperoxidase-oxidase substrates. *Biochem. J.* **1988**, *253*, 441–449.
- (23) Malle, E.; Furtmuller, P. G.; Sattler, W.; Obinger, C. Myeloperoxidase: a target for new drug development? *Br. J. Pharmacol.* **2007**, *152*, 838–854.
- (24) Hsuanyu, Y.; Dunford, H. B. Oxidation of clozapine and ascorbate by myeloperoxidase. *Arch. Biochem. Biophys.* **1999**, *368*, 413–420.
- (25) Forbes, L. V.; Furtmuller, P. G.; Khalilova, I.; Turner, R.; Obinger, C.; Kettle, A. J. Isoniazid as a substrate and inhibitor of myeloperoxidase: Identification of amine adducts and the influence of superoxide dismutase on their formation. *Biochem. Pharmacol.* **2012**, *84*, 949–960.
- (26) Kettle, A. J.; Maroz, A.; Woodroffe, G.; Winterbourn, C. C.; Anderson, R. F. Spectral and kinetic evidence for reaction of superoxide with compound I of myeloperoxidase. *Free Radical Biol. Med.* **2011**, *51*, 2190–2194.
- (27) Marquez, L. A.; Dunford, H. B. Kinetics of oxidation of tyrosine and dityrosine by myeloperoxidase compounds I and II. Implications for lipidprotein peroxidation studies. *J. Biol. Chem.* **1995**, *270*, 30434–30440.
- (28) Meotti, F. C.; Jameson, G. N.; Turner, R.; Harwood, D. T.; Stockwell, S.; Rees, M. D.; Thomas, S. R.; Kettle, A. J. Urate as a physiological substrate for myeloperoxidase: implications for hyperuricemia and inflammation. *J. Biol. Chem.* **2011**, *286*, 12901–12911.
- (29) Kettle, A. J.; Gedye, C. A.; Winterbourn, C. C. Superoxide is an antagonist of anti-inflammatory drugs that inhibit hypochlorous acid production by myeloperoxidase. *Biochem. Pharmacol.* **1993**, *45*, 2003–2010.
- (30) Tiden, A. K.; Sjogren, T.; Svensson, M.; Bernlind, A.; Senthilmohan, R.; Auchere, F.; Norman, H.; Markgren, P. O.; Gustavsson, S.; Schmidt, S.; Lundquist, S.; Forbes, L. V.; Magon, N. J.; Paton, L. N.; Jameson, G. N.; Eriksson, H.; Kettle, A. J. 2-Thioxanthines are mechanism-based inactivators of myeloperoxidase that block oxidative stress during inflammation. *J. Biol. Chem.* **2011**, *286*, 37578–37589.
- (31) Geoghegan, K. F.; Varghese, A. H.; Feng, X.; Bessire, A. J.; Conboy, J. J.; Ruggeri, R. B.; Ahn, K.; Spath, S. N.; Filippov, S. V.; Conrad, S. J.; Carpino, P. A.; Guimaraes, C. R.; Vajdos, F. F. Deconstruction of activity-dependent covalent modification of heme in human neutrophil myeloperoxidase by multistage mass spectrometry (MS(4)). *Biochemistry* **2012**, *51*, 2065–2077.
- (32) Ward, J.; Spath, S. N.; Pabst, B.; Carpino, P. A.; Ruggeri, R. B.; Xing, G.; Speers, A. E.; Cravatt, B. F.; Ahn, K. Mechanistic characterization of a 2-thioxanthine myeloperoxidase inhibitor and selectivity assessment utilizing click chemistry – activity-based protein profiling. *Biochemistry* **2013**, *52*, 9187–9201.
- (33) Fumarola, A.; Di Fiore, A.; Dainelli, M.; Grani, G.; Calvanese, A. Medical treatment of hyperthyroidism: state of the art. *Exp. Clin. Endocrinol. Diabetes* **2010**, *118*, 678–684.
- (34) Lee, E.; Hirouchi, M.; Hosokawa, M.; Sayo, H.; Kohno, M.; Kariya, K. Inactivation of peroxidases of rat bone marrow by repeated administration of propylthiouracil is accompanied by a change in the heme structure. *Biochem. Pharmacol.* **1988**, *37*, 2151–2153.
- (35) Lee, E.; Miki, Y.; Katslira, H.; Kariya, K. Mechanism of inactivation of myeloperoxidase by propylthiouracil. *Biochem. Pharmacol.* **1990**, *39*, 1467–1471.
- (36) Jiang, X.; Khursigara, G.; Rubin, R. L. Transformation of lupus-inducing drugs to cytotoxic products by activated neutrophils. *Science* **1994**, *266*, 810–813.
- (37) Waldhauser, L.; Uetrecht, J. Oxidation of propylthiouracil to reactive metabolites by activated neutrophils. Implications for agranulocytosis. *Drug Metab. Dispos.* **1991**, *19*, 354–359.
- (38) Copeland, R. A. Evaluation of enzyme inhibitors in drug discovery. A guide for medicinal chemists and pharmacologists. *Methods Biochem. Anal.* **2005**, *46*, 1–265.
- (39) Zheng, W.; Warner, R.; Ruggeri, R. B.; Su, C.; Cortes, C.; Skoura, A.; Ward, J.; Ahn, K.; Kalgutkar, A.; Sun, D.; Maurer, T.; Bonin, P.; Okerberg, C.; Bobrowski, W.; Kawabe, T. T.; Zhang, Y.; Coskran, T. M.; Bell, S.; Kapoor, B.; Johnson, K.; Buckbinder, L. PF-1355, a mechanism-based myeloperoxidase inhibitor, prevents immune-complex vasculitis and anti-glomerular basement membrane glomerulonephritis. *J. Pharmacol. Exp. Ther.* **2015**, *353*, 288–298.
- (40) Neidlein, R.; Menche, G. Synthese von 3,4-sowie 4-substituierten uracilen und thiouracilen. *Arch. Pharm.* **1972**, *305*, 596–601.
- (41) Medda, F.; Joseph, T. L.; Pirrie, L.; Higgins, M.; Slawin, A. M. Z.; Lain, S.; Verma, C.; Westwood, N. J. N1-Benzyl substituted cambinol analogues as isozyme selective inhibitors of the sirtuin family of protein deacetylases. *MedChemComm* **2011**, *2*, 611–615.
- (42) Kalgutkar, A. S.; Gardner, I.; Obach, R. S.; Shaffer, C. L.; Callegari, E.; Henne, K. R.; Mutlib, A. E.; Dalvie, D. K.; Lee, J. S.; Nakai, Y.; O'Donnell, J. P.; Boer, J.; Harriman, S. P. A comprehensive listing of bioactivation pathways of organic functional groups. *Curr. Drug Metab.* **2005**, *6*, 161–225.
- (43) Fitcher, P. H.; Massie, E. Agranulocytosis due to propylthiouracil. *Ann. Intern. Med.* **1950**, *32*, 137.
- (44) Cooper, D. S. Antithyroid drugs. *N. Engl. J. Med.* **2005**, *352*, 905–917.
- (45) Ichiki, Y.; Akahoshi, M.; Yamashita, N.; Morita, C.; Maruyama, T.; Horiuchi, T.; Hayashida, K.; Ishibashi, H.; Niho, Y. Propylthiouracil-induced severe hepatitis: a case report and review of the literature. *J. Gastroenterol.* **1998**, *33*, 747–750.
- (46) Guffy, M. M.; Goeken, N. E.; Burns, C. P. Granulocytotoxic antibodies in a patient with propylthiouracil-induced agranulocytosis. *Arch. Intern. Med.* **1984**, *144*, 1687–1688.
- (47) Fibbe, W. E.; Claas, F. H.; Van der Star-Dijkstra, W.; Schaafsma, M. R.; Meyboom, R. H.; Falkenburg, J. H. Agranulocytosis induced by propylthiouracil: evidence of a drug dependent antibody reacting with granulocytes, monocytes and haematopoietic progenitor cells. *Br. J. Haematol.* **1986**, *64*, 363–373.
- (48) Bilezikian, S. B.; Laleli, Y.; Tsan, M. F.; Hodgkinson, B. A.; Ice, S.; McIntyre, P. A. Immunological reactions involving leukocytes: III. Agranulocytosis induced by antithyroid drugs. *Johns Hopkins Med. J.* **1976**, *138*, 124–129.
- (49) Berkman, E. M.; Orlin, J. B.; Wolfsdorf, J. An anti-neutrophil antibody associated with a propylthiouracil-induced lupus-like syndrome. *Transfusion* **1983**, *23*, 135–138.

(50) Kitamura, I. R. The action of hydrogen peroxide on organic sulfur compounds. *Yakugaku Zasshi* **1934**, *54*, 1–13.

(51) Kalm, M. J. Peroxide desulfurization of thioureas. *J. Org. Chem.* **1961**, *26*, 2925–2929.

(52) Henderson, M. C.; Siddens, L. K.; Krueger, S. K.; Stevens, J. F.; Kedzie, K.; Fang, W. K.; Heidelbaugh, T.; Nguyen, P.; Chow, K.; Garst, M.; Gil, D.; Williams, D. E. Flavin-containing monooxygenase S-oxygenation of a series of thioureas and thiones. *Toxicol. Appl. Pharmacol.* **2014**, *278*, 91–99.

(53) Henderson, M. C.; Krueger, S. K.; Stevens, J. F.; Williams, D. E. Human flavin-containing monooxygenase form 2 S-oxygenation: sulfenic acid formation from thioureas and oxidation of glutathione. *Chem. Res. Toxicol.* **2004**, *17*, 633–640.

(54) Mansuy, D.; Dansette, P. M. Sulfenic acids as reactive intermediates in xenobiotic metabolism. *Arch. Biochem. Biophys.* **2011**, *507*, 174–185.

(55) Stopher, D.; McClean, S. An improved method for the determination of distribution coefficients. *J. Pharm. Pharmacol.* **1990**, *42*, 144.

(56) Korolev, D.; Balakin, K. V.; Nikolsky, Y.; Kirillov, E.; Ivanenkov, Y. A.; Savchuk, N. P.; Ivashchenko, A. A.; Nikolskaya, T. Modeling of human cytochrome p450-mediated drug metabolism using unsupervised machine learning approach. *J. Med. Chem.* **2003**, *46*, 3631–3643.

(57) Di, L.; Whitney-Pickett, C.; Umland, J. P.; Zhang, H.; Zhang, X.; Gebhard, D. F.; Lai, Y.; Federico, J. J., 3rd; Davidson, R. E.; Smith, R.; Reyner, E. L.; Lee, C.; Feng, B.; Rotter, C.; Varma, M. V.; Kempshall, S.; Fenner, K.; El-Kattan, A. F.; Liston, T. E.; Troutman, M. D. Development of a new permeability assay using low-efflux MDCKII cells. *J. Pharm. Sci.* **2011**, *100*, 4974–4985.

(58) Banker, M. J.; Clark, T. H.; Williams, J. A. Development and validation of a 96-well equilibrium dialysis apparatus for measuring plasma protein binding. *J. Pharm. Sci.* **2003**, *92*, 967–974.

(59) Walsky, R. L.; Obach, R. S. Validated assays for human cytochrome P450 activities. *Drug Metab. Dispos.* **2004**, *32*, 647–660.

(60) Orr, S. T.; Ripp, S. L.; Ballard, T. E.; Henderson, J. L.; Scott, D. O.; Obach, R. S.; Sun, H.; Kalgutkar, A. S. Mechanism-based inactivation (MBI) of cytochrome P450 enzymes: structure-activity relationships and discovery strategies to mitigate drug-drug interaction risks. *J. Med. Chem.* **2012**, *55*, 4896–4933.

(61) Varma, M. V.; Feng, B.; Obach, R. S.; Troutman, M. D.; Chupka, J.; Miller, H. R.; El-Kattan, A. Physicochemical determinants of human renal clearance. *J. Med. Chem.* **2009**, *52*, 4844–4852.

(62) Taylor, F. B.; Haddad, P. A.; Hack, E.; Chang, A. C.; Peer, G. T.; Morrissey, J. H.; Li, A.; Allen, R. C.; Wada, H.; Kinasewitz, G. T. Two-stage response to endotoxin infusion into normal human subjects: Correlation of blood phagocyte luminescence with clinical and laboratory markers of the inflammatory, hemostatic response. *Crit. Care Med.* **2001**, *29*, 326–334.

(63) Obach, R. S. Predicting clearance in humans from in vitro data. *Curr. Top. Med. Chem.* **2011**, *11*, 334–339.